RECENT VELOCITY FIELD IN EASTERN ANATOLIA FROM A COMBINATION OF CONTINUOUS AND CAMPAIGN TYPE GPS OBSERVATION

by

Ömer Farisoğulları

B.S., Geodesy and Photogrammetry Engineering, Yıldız Technical University, 2008

Submitted to Kandilli Observatory and Earthquake Research Institute,

in partial fulfillment of the requirements for the degree of

Master of Science

Graduate Program in Geodesy

Boğaziçi University

2013

RECENT VELOCITY FIELD IN EASTERN ANATOLIA FROM A COMBINATION OF CONTINUOUS AND CAMPAIGN TYPE GPS OBSERVATION

APPROVED BY:

Prof. Dr. Haluk ÖZENER . . . . . .

(Thesis Supervisor)

Assoc. Prof. Dr. Bahadır AKTUĞ . . . . . .

Assoc. Prof. Dr. Uğur DOĞAN . . . . . .

(Yıldız Technical University)

DATE OF APPROVAL: 27.05.2013

ACKNOWLEDGEMENTS

This study is realized with many valuable contributions. First of all I would like to thank to my supervisor, Prof. Dr. Haluk Özener for his great support, guidance and encouragement in this study.

I am grateful to the members of the jury, Assoc. Prof. Dr. Bahadır Aktuğ and Assoc. Prof. Dr. Uğur Doğan for their advices, and comments. I want to express my special thanks to Assoc. Prof. Dr. Bahadır Aktuğ for their help, support, interest and valuable hints.

I am also thankful to Assoc. Prof. Dr. Aslı Doğru, Dr. Onur Yılmaz and Eng. Bülent Turgut for sharing the experience and during the processing of data.

I also want to thank to Res. Assist. Emre Havazlı, M.Sc. Kerem Halıcıoğlu and Res. Assist. Aslı Sabuncu for their help, guidance and encouragement.

Finally, I am very grateful to my family for their great trust and support and all my dear friends.

ABSTRACT

RECENT VELOCITY FIELD IN EASTERN ANATOLIA FROM A COMBINATION OF CONTINUOUS AND CAMPAIGN TYPE GPS OBSERVATION

The tectonic structure of our country is the result of collision of Arabian, African and Eurasian plates. Deformation towards to the west of the Karlıova region, which is the conjunction of North Anatolian Fault Zone with East Anatolian Fault Zone, is caused by the strike-slip faulting along North Anatolian Fault Zone and East Anatolian Fault Zone and the deformation from this intersection area to the east is caused by the thrust faults exist in the region.

In Eastern Turkey, many scientific studies have been conducted with applying geodetic methods. In this study, six epochs of data from 19 of CORS-TR stations were used and data was chosen by considering seasonal effects. GAMIT/GLOBK academic software was used to process the data and obtain velocity field of the study area.

The obtained velocities of stations were combined with the velocity fields of Reilinger *et al*., (2006) and Aktuğ *et al*., (2013). The transformation process is performed by using 13 IGS stations which are mutual in the studies. Obtained velocity values vary between 3.77 mm/yr ±0.52 mm/yr and 24.94 mm/yr ±5.34 mm/yr.

The results obtained show consistency with the recent tectonic structure of the region. The results of prior studies in the study area is considered and taken into account within the processing of data which made it possible to consider a long term data set. Long term data set allowed obtaining the velocity field of the area more accurately.

ÖZET

SÜREKLİ VE KAMPANYA TİPİ GPS GÖZLEMLERİNİN BİRLEŞTİRİLMESİ İLE DOĞU ANADOLU' NUN GÜNCEL HIZ ALANININ BELİRLENMESİ

Ülkemizin içinde bulunduğu bölgenin tektonik yapısı; Arap, Afrika ve Avrasya levhalarının çarpışması ile oluşmaktadır. Kuzey Anadolu ve Doğu Anadolu Fay Zonları boyunca gerçekleşen doğrultu-atımlı faylanma, bu iki sistemin kesişiminde bulunan Karlıova bölgesindeki batıya doğru deformasyonu biçimlendirmekte ve bu kesişimden doğuya doğru olan deformasyon ise bölgede bulunan çok sayıdaki bindirme faylarının dağılımı ile tanımlanmaktadır.

Türkiye'nin doğusunda jeodezik yöntemler kullanılarak, birçok bilimsel çalışma yapılmıştır. Bu çalışmada ise, mevsimsel etkiler de göz önünde bulundurularak, sürekli gözlem yapan 19 adet CORS-TR istasyonundan 6 epok veri alınmış ve bu veriler GAMIT/GLOBK akademik yazılımı kullanılarak değerlendirilmiş ve hız değerleri elde edilmiştir.

Elde edilen hız değerleri, Reilinger *et al*., (2006) ve Aktuğ *et al*., (2013) hızlarıyla birleştirilmiştir. Dönüşüm işlemi, ortak olarak belirlenen 13 adet IGS istasyonu kullanılarak yapılmıştır. Birleştirme sonucu elde edilen hız değerleri, 3.77 mm/yıl ±0.52 mm/yıl ile 24.94 mm/yıl ±5.34 mm/yıl arasında değişmektedir.

Elde edilen sonuçların bölgenin güncel tektonik yapısı ile uyumlu olduğu belirlenmiştir. Geçmişte yapılmış olan çalışmaların sonuçları da göz önünde bulundurularak, çalışmamızda elde ettiğimiz sonuçlar ile birlikte değerlendirilmiş ve böylelikle geniş bir zaman aralığındaki veri setinden faydalanılmıştır. Geniş zaman aralığında toplanmış olan veriler, bölgenin güncel tektonik yapısı ile ilgili olarak daha doğru sonuçlar elde etme imkânı sunmuştur.

TABLE OF CONTENTS

ACKNOWLEDGEMENTS..... iii

ABSTRACT..... iv

ÖZET..... v

LIST OF FIGURES..... viii

LIST OF TABLES..... xii

LIST OF SYMBOLS..... xiii

1. INTRODUCTION..... 1

2. TECTONIC SETTINGS OF TURKEY AND EAST ANATOLIA..... 5

2.1. Active Tectonics of the Study Area..... 8

3. CORS (CONTINUOUSLY OPERATING REFERENCE STATION) AND CORS-TR SYSTEM..... 13

3.1. GNSS CORS SYSTEM..... 13

3.1.1. CORS Techniques..... 16

3.1.1.1. FKP Area Correction Technique..... 16

3.1.1.2. VRS Technique..... 17

3.1.1.3. MAC Technique..... 18

3.1.2. CORS and GNSS Principles and Comparision 19

3.1.3. Benchmark Tests..... 21

3.2. GNSS CORS-TR System. 23

3.2.1. CORS-TR Design..... 24

3.2.2. CORS-TR Establishment..... 26

3.2.3. Control Center..... 27

3.2.4. Central Processing Systems..... 28

3.2.5. Reference Stations..... 29

3.2.6. CORS-TR Positioning Users..... 30

3.2.7. CORS-TR Scientific Users..... 31

3.3. Data Used in Case Study..... 33
3.4. Selection of Software..... 36
3.4.1. GNSS CORS-TR Data Analyzing Software..... 36
3.4.2. GNSS Data Analyzing Strategies..... 38
3.4.3. Kalman Filter..... 39
3.5. CORS-TR Data Processing Results..... 43
3.6. Combine Velocity Field..... 45
4. RESULTS AND DISCUSSION..... 53
REFERENCES..... 56
APPENDIX A..... 66

LIST OF FIGURES

Figure 1.1. Major plates of the Earth taken from Helland, (2005) 2

Figure 1.2. CORS-TR reference stations in East Anatolia..... 3

Figure 2.1. Tectonic setting of Turkey and surrounding regions..... 5

Figure 2.2. Map showing the NAFZ and EAFZ in the region..... 7

Figure 2.3. Arabian-African-Eurasian plate interaction..... 9

Figure 2.4. Regional seismicity between 1903 and 2013 with magnitude larger than 4.0 10

Figure 3.1. GNSS satellites..... 15

Figure 3.2. Linear FKP planes for four reference stations..... 17

Figure 3.3. Classical and CORS Approach (Eren *et al*., 2009)..... 20

Figure 3.4. Benchmark test networks..... 22

Figure 3.5. CORS-TR reference stations and main faults in Turkey and Cyprus..... 24

Figure 3.6. CORS-TR System Design..... 25

Figure 3.7. Antenna Types used in CORS-TR Reference Stations 26

Figure 3.8. Master Control Station and its schematic representation..... 27

Figure 3.9. Use of CORS-TR VRS..... 28

Figure 3.10. The network of CORS-TR stations..... 30

Figure 3.11. CORS-TR Applications..... 31

Figure 3.12. Velocity vectors with respect to Eurasian Plate..... 32

Figure 3.13. CORS-TR Stations in Study Area..... 33

Figure 3.14. Trimble NetR5 GNSS CORS receiver..... 35

Figure 3.15. Horizontal GPS velocities in Eurasia-fixed frame and confidence ellipses plotted with 95 %..... 43

Figure 3.16. GPS velocities from Reilinger *et al.,* (2006) in blue, Aktuğ *et al.,* (2013) in red and CORS-TR in green..... 52

Figure 4.1. GPS velocities from Reilinger *et al.,* (2006) and Özener *et al.,* (2010)..... 54

Figure A.1. AGRD station and its coordinate-time series..... 67

Figure A.2. ARPK station and its coordinate-time series..... 68

Figure A.3. BAYB station and its coordinate-time series..... 69

Figure A.4. BING station and its coordinate-time series..... 70

Figure A.5. DIVR station and its coordinate-time series..... 71

Figure A.6. ELAZ station and its coordinate-time series..... 72

Figure A.7. ERGN station and its coordinate-time series..... 73

Figure A.8. ERZI station and its coordinate-time series..... 74

Figure A.9. ERZR station and its coordinate-time series..... 75

Figure A.10. GUMU station and its coordinate-time series..... 76

Figure A.11. HINI station and its coordinate-time series..... 77

Figure A.12. HORS station and its coordinate-time series..... 78

Figure A.13. MALZ station and its coordinate-time series..... 79

Figure A.14. MUUS station and its coordinate-time series..... 80

Figure A.15. RHIY station and its coordinate-time series..... 81

Figure A.16. SSEH station and its coordinate-time series..... 82

Figure A.17. TNCE station and its coordinate-time series..... 83

Figure A.18. TVAN station and its coordinate-time series..... 84

Figure A.19. UDER station and its coordinate-time series..... 85

LIST OF TABLES

Table 2.1. Regional seismicity between 1903 and 2013 with magnitude larger than 6.0.. 12

Table 3.1. CORS Network Distance (Eren *et al*., 2007)..... 21

Table 3.2. Coordinates of CORS-TR reference stations used fully study..... 34

Table 3.3. CORS-TR reference stations dates and observation duration..... 35

Table 3.4. Scientific GPS data processing software and supporting institutions..... 36

Table 3.5. Summary of velocity estimates in Eurasia fixed reference frame..... 44

Table 3.6. The common sites used in the transformation..... 46

Table 3.7. Estimated Euler Pole in geographic units..... 47

Table 3.8. Estimated Euler Pole in angular vector units..... 47

Table 3.9. The CORS-TR velocities..... 48

Table 3.10. The velocities given in Aktuğ *et al.,* (2013)..... 49

Table 3.11. The velocities given in Reilinger *et al.,* (2006)..... 50

Table 3.12. The combined velocities..... 51

LIST OF SYMBOLS / ABBREVIATIONS

GPS	Global Positioning System
KOERI	Kandilli Observatory and Earthquake Research Institute
ITRF	International Terrestrial Reference Frame
NAFZ	North Anatolian Fault Zone
EAFZ	East Anatolian Fault Zone
KTJ	Karlıova Triple Junction
GNSS	Global Navigation Satallite System
CORS-TR	Continuous Operating Reference Station in Turkey
NE	North East
OF	Ovacık Fault
PF	Pülümür Fault
YS	Yedisu Segment
NAFZ	North Anatolian Fault System
EAFS	East Anatolian Fault System
FKP	Flachen Korrectur Parameter
VRS	Virtual Reference Stations
MAC	Master Auxiliary Concept
RTCM	Real Time Correction Message
RTK	Real Time Kinematic
BM	Benchmark Test
GDLRC	General Directorate of Land Registry and Cadastre
IKU	İstanbul Kültür University
GCM	General Command of Mapping
ED50	European Datum-1950
TUBITAK	Scientific and Technological Research Council of Turkey
CC	Control Center

NTRIP	Network Transport of RTCM through Internet Protocol
DGPS	Differential Global Positioning System
GIS	Geographic Information Service
LIS	Land Information Service
AGRD	Ağrı
ARPK	Arapkir
BAYB	Bayburt
BING	Bingöl
DIVR	Divriği
ELAZ	Elazığ
ERGN	Ergani
ERZI	Erzincan
ERZR	Erzurum
GUMU	Gümüşhane
HINI	Hınıs
HORS	Horasan
MALZ	Malazgirt
MUUS	Muş
RHIY	Reşadiye
SSEH	Suşehri
TVAN	Tatvan
TNCE	Tunceli
UDER	Uzundere
VLBI	Very Long Base Interferometry
SLR	Satellite Laser Ranging
IGS	International GNSS Service
SOPAC	Scripps Orbit and Permanent Array

1. INTRODUCTION

The eastern Mediterranean, the Middle East, and northeast Africa is a zone of complex tectonics related with the interaction of three of the Earth's major lithospheric plates, Arabia, Africa, and Eurasia (Figure 1.1) (McKenzie 1970, 1972).

During the middle Miocene (23-5.5 Millions years ago), Arabia was separated from Africa along the left-lateral Dead Sea fault zone (Le Pichon *et al*., 1988). In the middle to late Miocene time interval, the northern border of Arabia entered into collision with the southern margin of Eurasia, forming the Bitlis Thrust Zone. In the mean time, the African plate is subducting under the Anatolian and Aegean plates by creating Hellenic Arc (Le Pichon *et al*., 1988).

Therefore, along the Hellenic Trench, northeastern part of Africa moves approximately 10 mm/yr towards North while northern Arabian plate has been slowly moving northwest with a velocity of 18-25 mm/yr relative to Eurasia (McClusky *et al*., 2000).

Turkey is situated on Anatolian plate where the Arabian, Eurasian and the African plates conjunct. The recent studies displayed that the Anatolian plate has been pressed by Eurasian and Arabian plates due to the worldwide plate tectonics. Anatolian plate is rotating counter-clockwise, relative to Eurasia which results in a slip velocity of 24 mm/yr in the North Anatolian Fault (McClusky *et al*., 2000).

Anatolian plate, being under the impact of these large plates, moves westwards. The collision between Eurasia and Arabian plate has been realized as the main force for this movement (Şengör *et al*., 2005). On the other hand, it is also suggested that the increasing rate of motion toward the Hellenic and Cyprus ditches has been accountable for the westward motion of Anatolia (Reilinger *et al*., 2006).

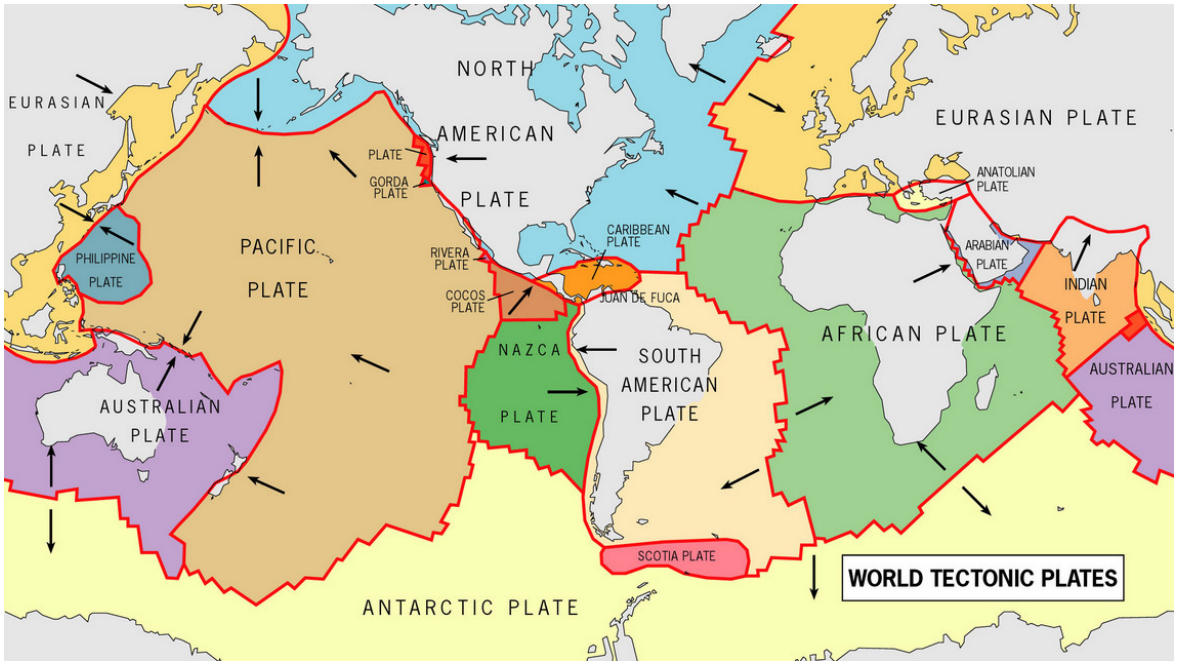

Figure 1.1. Major plates of the Earth taken from Helland, (2005).

The study area, where the NAFZ and East Anatolian Fault Zone (EAFZ) cross with Karlıova Triple Junction (KTJ) in eastern Turkey, contains a complex combining of active plate boundaries.

North Anatolian Fault Zone (NAFZ) is one of the major strike-slip fault zones of the world. The 1200 km-long NAFZ runs along the northern part of Turkey nearly parallel to the Black Sea from Karlıova in the east to the Gulf of Saros in the west, connecting the East Anatolian compressional region to the Aegean extensional region (Özener *et al.*, 2010).

The East Anatolian Fault Zone (EAFZ) is one of the major elements in this tectonic framework representing a left-lateral strike-slip plate boundary extending over approximately 500 km between the Arabian and Anatolian plates in eastern Turkey.

The EAFZ comprises several obvious strands with localized pull-apart basins and push-up zones rather than a throughgoing continuous fault plane (Şengör *et al.*, 1985; Emre and Duman, 2007).

Based on fault geometry and strike of the strands, the EAFZ consists of five (Hempton *et al*., 1981) or six segments (Saroğlu *et al*., 1992). The age of the fault zone remains to be controversial, but it likely formed between Late Miocene-Early Pliocene (Şengör *et al*., 1985; Hempton, 1987) to Late Pliocene (Emre and Duman, 2007).

The current slip rate across the EAFZ varies between 6 and 10 mm/year following different measurement techniques (seismic moments of earthquakes (Taymaz *et al*., 1991); GPS measurements (McClusky *et al*., 2000). Left-lateral displacement along the EAFZ is also confirmed by seismological observations (McKenzie, 1972; Taymaz *et al*., 1991) and geological studies (Saroğlu *et al*., 1992).

Turkey has significant earthquake-resistant design provisions and codes. However, it is also valuable to have systems that run continuously to observe the tectonic plate movements, it is also useful tool for estimation of ground motions. This study aims to combine velocities of CORS-TR stations and GPS campaigns so it gives a better understanding in the monitoring of the tectonic plate movements in eastern Anatolia (Figure 1.2).

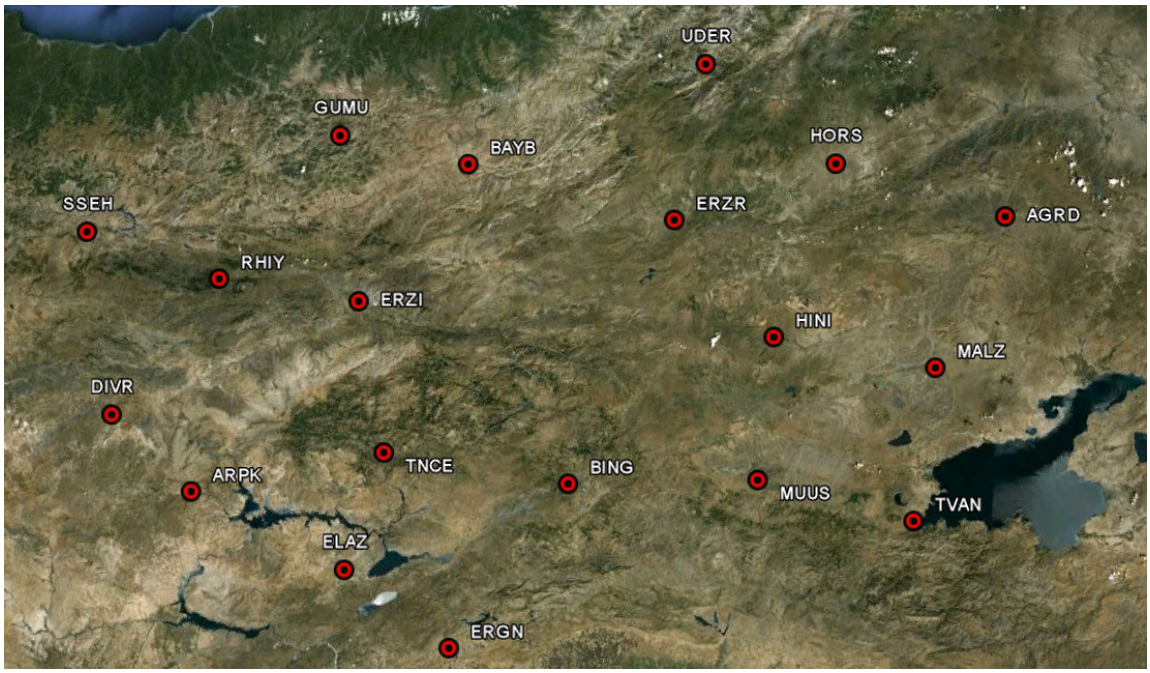

Figure 1.2. CORS-TR reference stations in East Anatolia.

Geodetic techniques for monitoring the displacements and the deformation parameters are recognized as a favorable method in many studies focused on crustal movements.

This study has four chapters. The second chapter of this study explains the seismicity and tectonics of the region. Besides, significant faults in the region and their locations are explained and indicated with maps in the study area. North Anatolian Fault Zone (NAFZ), East Anatolia Fault Zone (EAFZ), Karlıova Triple Junction (KTJ) in eastern Turkey and their properties are introduced in details. Additionally, historical and instrumental period of earthquake records are placed in this chapter.

The third chapter of the study explains the fundamentals of CORS-TR reference stations. The data analyzing strategies and the GAMIT/GLOBK software is also explained in this chapter.

The fourth chapter gives the calculation methods, comparison and results.

2. TECTONIC SETTINGS OF TURKEY AND EASTERN ANATOLIA

Forming the boundary of the Eurasian and Anatolian tectonic plates, the NAFZ is one of the major strike-slip fault zones of the world. The 1200 km-long NAFZ runs along the northern part of Turkey, roughly parallel to the Black Sea from Karlıova in the east to the Gulf of Saros in the west, connecting the East Anatolian compressional region to the Aegean extensional region. NAFZ and EAFZ chance upon at Karlıova Triple Junction in eastern Turkey, comprises a complicated combination of active plate boundaries (Özener *et al*., 2010). Şengör *et al*., (1985) and Dewey *et al*., (1986) supposed that is due to the northward movement of the Arabian plate relative to Eurasia. The Erzincan–Karlıova region is crushed and squeezed westward along the NAFZ and EAFZ (Figure 2.1).

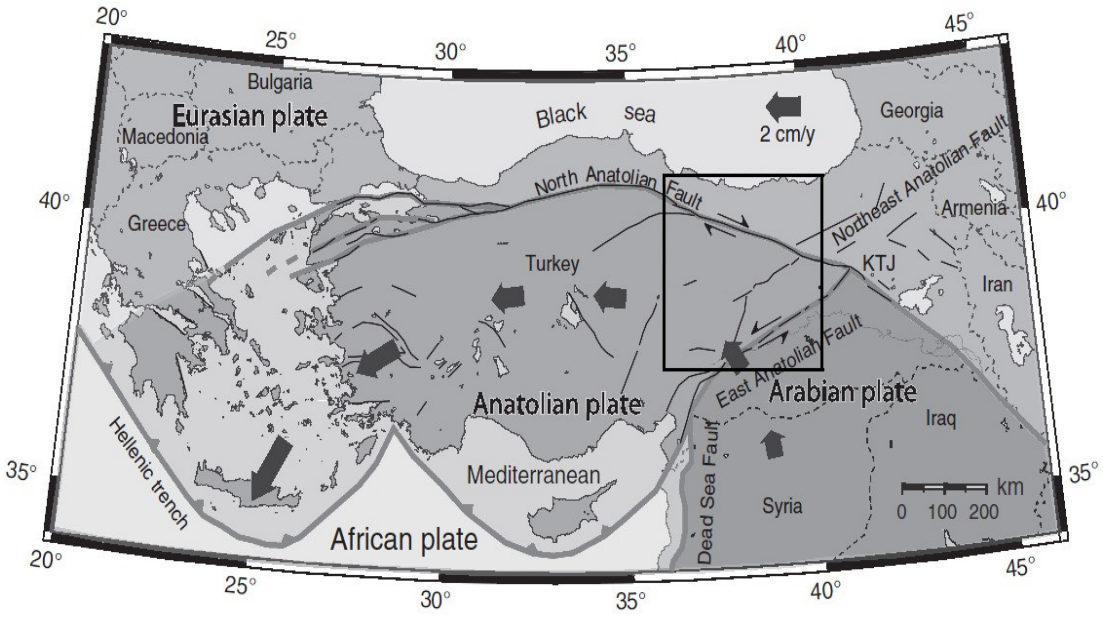

Figure 2.1. Tectonic setting of Turkey and surrounding regions. Arrows show the counter clockwise rotation of the Arabian and Anatolian plates with respect to the Eurasian reference frame increasing westward (McClusky *et al*., 2000). Thin black lines show active faults (Saroğlu *et al*., 1992).

As a result of this plate convergence, right-lateral strike-slip faulting along the NAFZ (Dewey and Şengör, 1979; McClusky *et al*., 2000) and left-lateral strike-slip faulting along the EAFZ in eastern Turkey customizes the westward motion of Anatolia relative to Eurasia (Jackson and McKenzie, 1988; McKenzie, 1972; Tatar *et al*., 2004; Özener *et al*., 2010).

Global Positioning System (GPS) observations over the last two decades however bring out that slab pull along the Hellenic trench is the much driving force of Anatolia rather than the push caused by the collision of Eurasian and Arabian plate (McClusky *et al*., 2000; Oral, 1994; Reilinger *et al*., 1997, 2006).

Several geodynamic models have been offered to explicate the tectonics of the study area, where NAFZ and EAFZ join together. Reilinger et al., (2006) suggest that the principal boundary between the westward moving Anatolian plate and Arabia is currently characterized by left-lateral strike-slip (Özener *et al*., 2010).

In general, the NAFZ becomes wider from east to west (Şengör *et al*., 2005). While the zone is generally extremely narrow, barely wider than 10 km, (Herece and Akay, 2003) between Karlıova triple junction and Niksar basin in eastern Turkey it becomes a shear zone of a few hundred km wide around the Marmara region in northwest Turkey. The long-term geological slip rates have been predicted between 10 mm/year and 20.5 mm/year along different parts of the NAFZ, based on different geological, seismological and paleomagnetic methods (Barka and Kadinsky-Cade, 1988; Kasapoğlu and Toksöz, 1983; Kiratzi and Papazachos, 1995; Kozacı *et al*., 2007; Pınar *et al*., 1996; Piper *et al*., 1996; Taymaz *et al*., 1991).

The EAFZ is on average 30 km wide, and a 700 km long approximately NE-trending sinistral megashear located between Karlıova in the northeast and Karataş to Samandağ counties in the southwest (Arpat and Saroğlu, 1972; Koçyiğit *et al*., 2003).

North Anatolian Fault Zone (NAFZ) and East Anatolian Fault Zone (EAFZ) meet in the Karlıova triple junction in eastern Turkey comprises a complicated combination of active plate boundaries (Figure 2.2) (Şengör *et al*., 1981). The active strike-slip deformation along the North Anatolian Fault Zone (NAFZ) in the last century has attracted attention of scientists all around the world. Features like high seismic activity and westward migration of devastating earthquakes encouraged scientists to implement many kinds of projects and study the NAFZ by using a wide range of observation methods. The EAFZ is not so well known as the NAFZ, although it has similar deformational characteristics and seismicity. A number of detailed geological and seismological works have been carried out on the EAFZ (Reilinger *et al*., 1997; Ambraseys and Jackson, 1998; Rojay *et al*., 2001; Nalbant *et al*., 2002; Gürsoy *et al*., 2003; Koçyiğit *et al*., 2003).

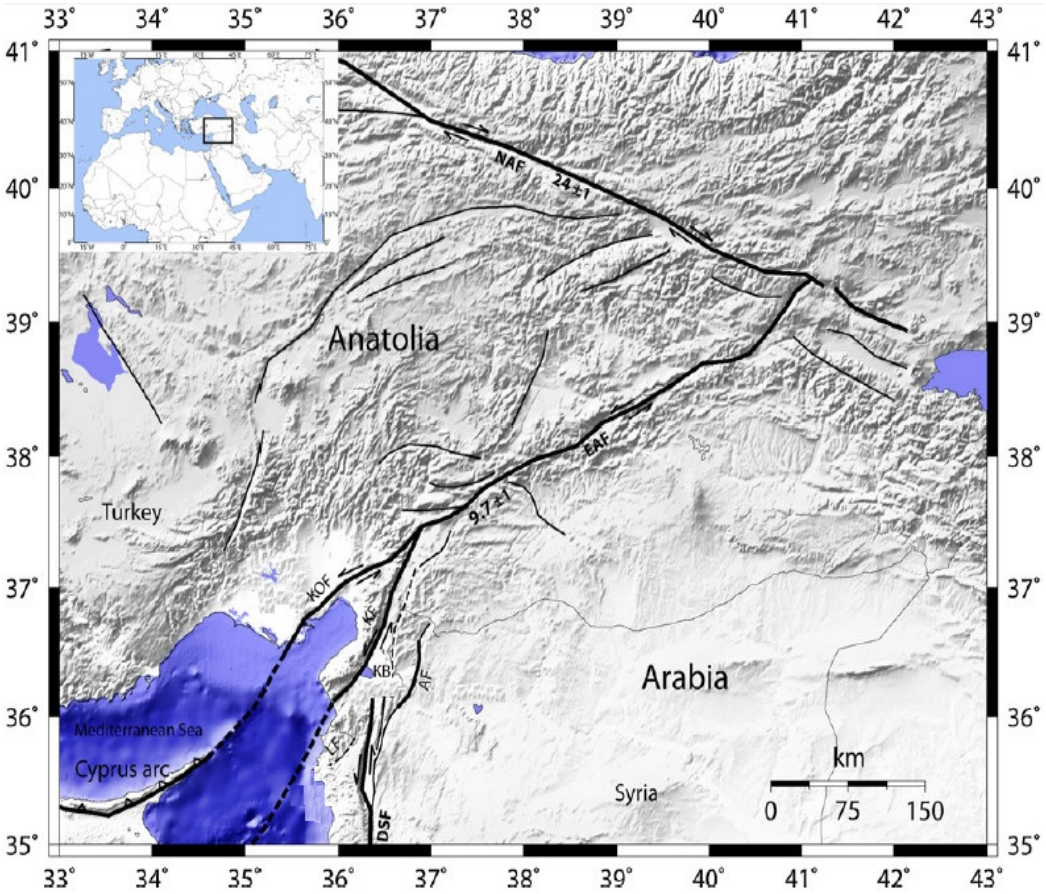

Figure 2.2. Map showing the NAFZ and EAFZ in the region taken from Meghraoui *et al*., (2011).

2.1. Active Tectonics of the Study Area

Anatolian plate is squeezed by the displacement of Eurasia, Africa and Arabian plates. Anatolian plate contains North Anatolian Fault Zone (NAFZ) and East Anatolian Fault Zone (EAFZ) (Doğru, 2010). The East Anatolian plate is approximately 2 km of average elevation and in many studies it can be thought of as a younger version of the Tibetan plateau (Şengör and Kidd, 1979; Dewey *et al*., 1986).

The Bitlis suture zone and the East Anatolian Fault Zone (EAFZ) show a disrupted, disordered, and active continental collision zone. The northward movement of the Arabian plate relation to Eurasia leads to lateral movement and rotation of the Anatolian block to the West. North Anatolian Fault Zone (NAFZ) displays the right-lateral strike-slip movement (Şengör, 1979; Dewey and Şengör, 1979; McClusky *et al*., 2000) and the left lateral strike-slip movement along the EAF (Figure 2.3) (McKenzie, 1972; Jackson and McKenzie, 1988). The Anatolian plate runs off westward due to the northward movement of the Arabian plate.

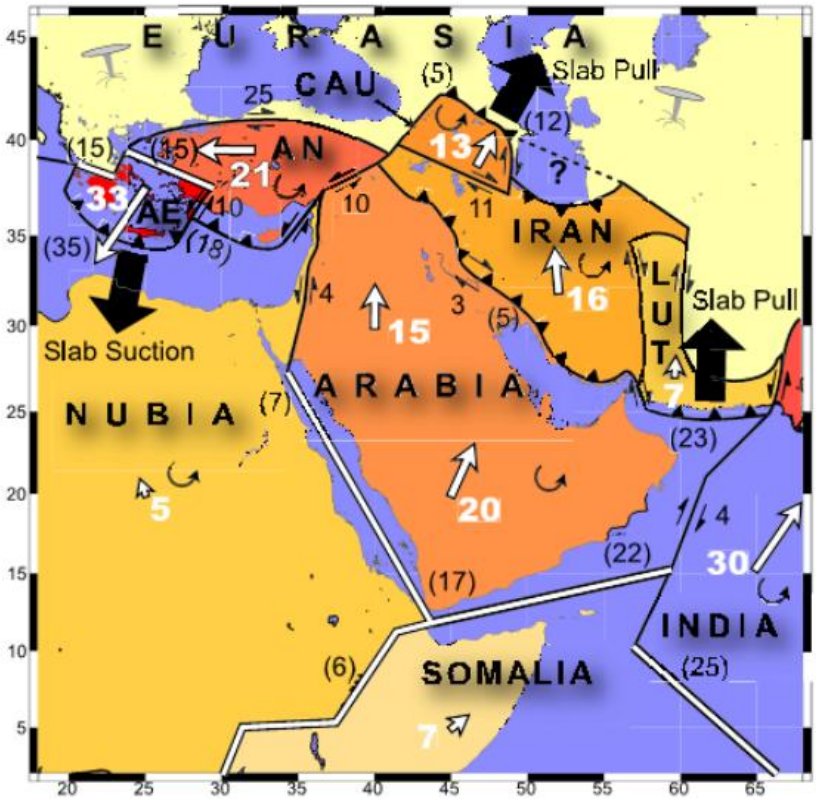

Figure 2.3. CAUC is the Caucasus block, AN is the Anatolian plate and AE is the Aegean plate. Double lines indicate extensional plate boundaries, lines with triangles indicate trust faults and plain lines show strike-slip boundaries. White arrows and adjacent numbers show GPS-derived plate velocities relative to the Eurasia in millimeters per year (Reilinger *et al.*, 2006).

The NAFZ and EAFZ have been active since the Miocene (23 – 5.5 Millions years ago), (Barka and Kadinsky-Cade, 1988) and are related with large pull apart basins, such as the Karlıova Basin located at the meeting of these two fault systems (Hempton, 1985).

The region to the east of Karlıova triple junction is represented by a N-S compressional tectonic regime and conjugate strike slip faults of dextral and sinistral character, mostly paralleling the North Anatolian Fault (NAF) and East Anatolian Fault (EAF) which are the dominant structural elements of the region. Historic records (Ambraseys, 1970, 1971) bring out that the EAFZ displays rarely large seismic activity (Arpat and Saroğlu, 1975; Özener *et al.*, 2010).

Since the beginning of the 20 th century, large earthquakes have been registered, providing precise information on their location and magnitudes, and these events affirm the fault lines mapped in that area (Figure 2.4).

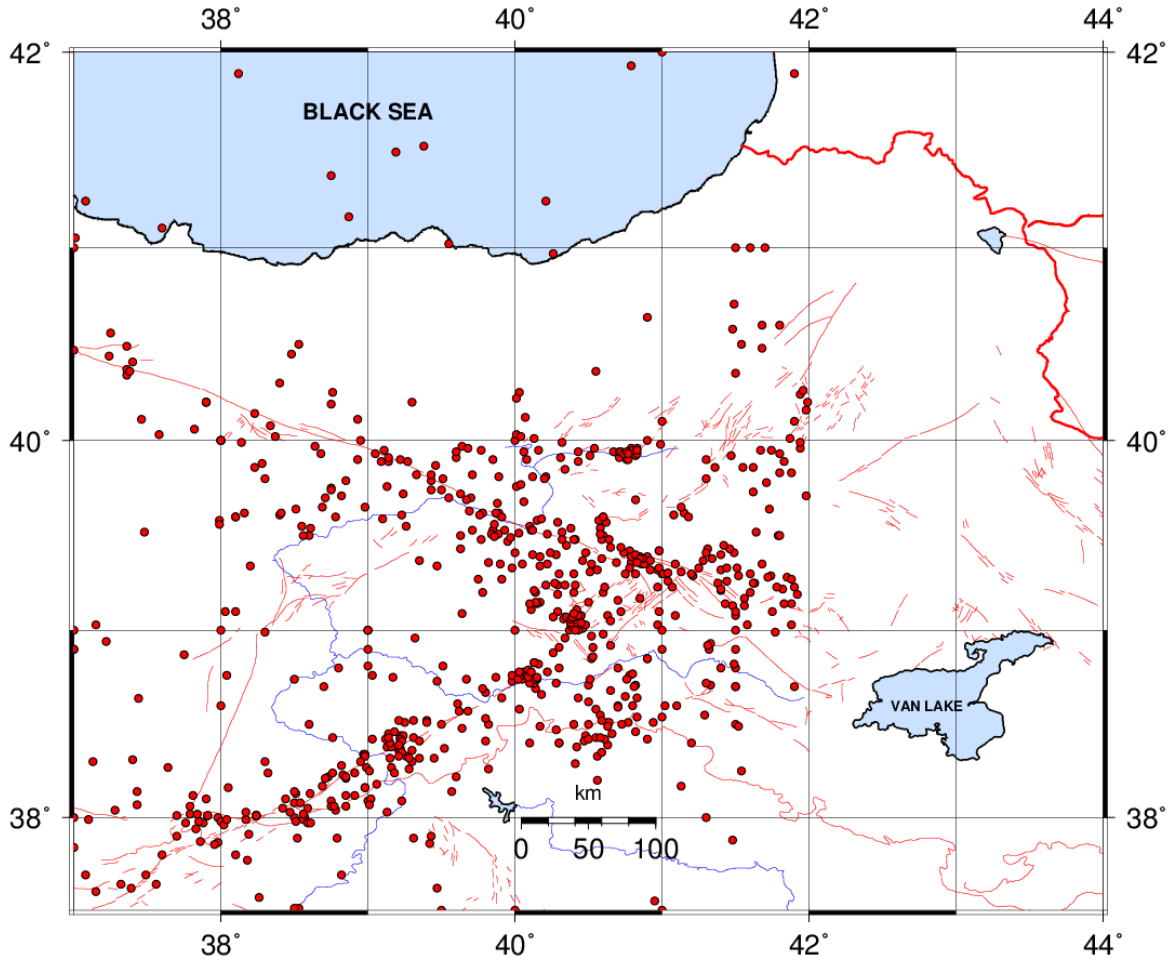

Figure 2.4. Regional seismicity between 1903 and 2013 with magnitude larger than 4.0 (KOERI - NEMC).

As shown in Figure 2.4 fault plane solution simply that the faulting type in the region is strike-slip faulting. Some of the earthquakes have dip-slip reverse normal faulting components.

A number of geodynamic models have been offered to explain the Arabia and Anatolia continental collision zone:

(a) continental subduction (Rotstein and Kafka, 1982),

(b) the Arabian plate convergence being suited wholly by microplate run off (McKenzie, 1976; Şengör and Kidd, 1979; Jackson and McKenzie, 1988),

(c) lithospheric thickening (Dewey *et al*., 1986), and

(d) lithospheric delamination (Pearce *et al*., 1990). It may be that a aggregation of these processes is taking place.

Rotstein and Kafka (1982) have recommended that the Arabian lithospheric plate is being subducted under the Eurasian plate at the Bitlis thrust zone based on the presence of evidently subcrustal earthquakes.

On the other hand, its southwestern maintenance to the Red Sea Fault or the Hellenic–Cyprus Arc is still beneath debate. Tirifonov (1995) indicated that the fault near the Karlıova Triple Junction was periodically moved by the NAF. Due to this offset, a few faults split in parallel at the southwestern part of the junction. Its southeastern branch is younger than the Northwestern branch.

The area to the east of the Karlıova Triple Junction (KTJ) is described by a N–S compressional tectonic regime where separated parts of continental lithosphere distorted comprised and produced a large bulk strain that has resulted in the generation of new construction or the reactivation of old construction (Bozkurt, 2001). The regime contrast between the east and the west of Karlıova, together with the large strain aggregation along the North Anatolian Fault Zone (NAFZ), makes the deformation surrounding the Karlıova Triple Junction (KTJ) crucial. The KTJ lies at the overlap of the Eurasian, Anatolian and Arabian plates, and is described by the North Anatolian Fault Zone (NAFZ) in the north and the East Anatolian Fault Zone (EAFZ) in the south.

A number of significant earthquakes occurred in the area during the last century, as defined in Table 2.1. The largest earthquake (magnitude 7.9) occurred in 1939 at Erzincan province, killing 32,968 people.

Table 2.1. Regional seismicity between 1903 and 2013 with magnitude larger than 6.0 (KOERI - NEMC).

	Longitude (deg)	**Magnitude (M)**	**Depth (km)**	**Date**
39.00	39.00	6.8	10	04.12.1905
40.50	42.00	6.0	10	28.12.1906
39.96	41.94	6.8	10	13.09.1924
39.80	39.51	7.9	20	26.12.1939
39.11	39.20	6.0	10	20.12.1940
39.74	39.50	6.0	10	08.11.1941
39.57	40.62	7.0	40	17.08.1949
38.13	38.51	6.0	3	14.06.1964
39.17	41.56	6.9	26	19.08.1966
39.42	40.98	6.2	14	20.08.1966
39.16	40.70	6.1	33	20.08.1966
39.54	40.38	6.2	30	26.07.1967
38.85	40.52	6.8	3	22.05.1971
38.51	40.77	6.6	32	06.09.1975
39.01	40.46	6.4	10	01.05.2003
38.80	40.10	6.0	5	08.03.2010

3. CORS (CONTINUOUSLY OPERATING REFERENCE STATION) AND CORS-TR SYSTEM

3.1. GNSS and CORS System

Geodesy relates with measuring the earth and creating best fit models for mapping or analyzing. More realistic models are created if the amount of data rises. Continuously observed measurements increase the productivity of the positioning systems. Continuous systems are analyzed through the viewpoint of Global Navigation Satellite Systems (GNSS). However, it should be noted that each data type could be designed to unsure continuous data.

In Continuously Operating Reference Station (CORS) concept, the GNSS Reference Stations are operating continuously on fixed sites. The most well known and significant network is International GNSS service (IGS) network. The IGS is dedicated to providing the highest quality GNSS data and products. However the new definition of CORS is different from these types of networks. IGS is continuous network but it is not a network operating actively for real-time or near real-time data outputs. The continuous data transfer from the receiver to a Server on which data assessment is continuously carried out differentiate active systems from the others. The accused data is stored by the Server system and analyzed in near real time to provide fast solutions for end users.

The CORS system is carried out globally, regionally or locally depending on the aim of the application. This means, the type of application designates the dimensions of the whole system including the control center and site. This also affects the futures of CORS receivers and infrastructure capacities.

GNSS-CORS Systems consist of GPS, GLONASS and GALILEO. Some information for each of these systems are provided below (Figure 3.1).

1. GPS, launch started in 1978 by United State of America (USA) and full configuration was completed in 1994. There are 31 GPS satellites. The GPS satellites broadcast the following radio waves:

    - L1, L2, L5 carrier frequencies
    - Additional, more capable military signals: M-code on L1 and L2
    - Additional, more capable civil signals: L2C, L5, L1C.

2. GLONASS, launch started in 1982 by Russia and full configuration is yet to be completed. The GPS satellites broadcast the following radio waves:

    - 3 allocated bands: G1 (1602 MHz), G2: (1245 MHz), G3 (1202 MHz)
    - C/A-like code: 511 chips, 1 ms code period, 50 bps data
    - All SVs use same PRN with frequency division multiple access (FDMA) using 16 frequency channels, reused for antipodal SVs.

3. GALILEO, launch started in 2005 and full configuration will be completed by 2014-2020. The GPS satellites broadcast the following radio waves:

    - L1, E1,E2,E5 and E6 signals.

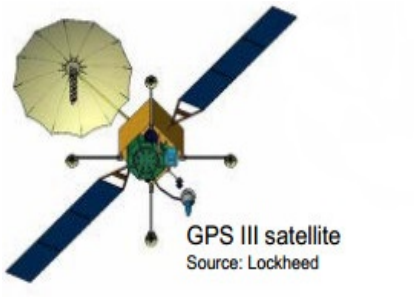

GPS

Launched: 1978

31 Satellite Constellation

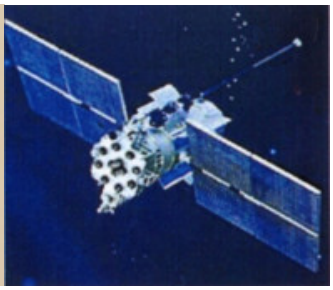

GLONASS

Launched: 1982

24 Working Satellite 2013

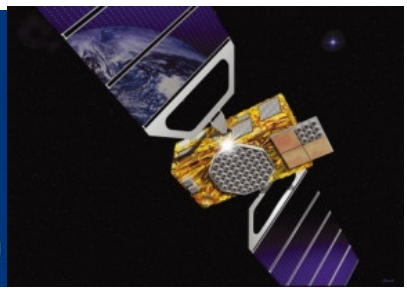

GALILEO

Launched: 2011-2012

4 in-orbit Validation Satellite

18 FOCs in orbit in 2014

Figure 3.1. GNSS satellites.

3.1.1. CORS Techniques

The observations from CORS stations are transmitted to the Control Center every second and corrections are computed after modeling atmospheric and other errors.

Three techniques are commonly used for CORS corrections to rovers:

- FKP correction
- VRS technique
- MAC technique

3.1.1.1. FKP Area Correction Technique. FKP is a means of representing the distance-dependent errors impressive an entire network in an additional message with a simple mathematical description plane. FKP is sent to rover by Control Center (CC) together with real corrections of nearest Reference Station.

In the technique known as Flachen Korrectur Parameter (FKP), atmospheric and/or phase corrections are computed in every CORS station (Wubbena *et al*., 2001; Vollath *et al*., 2000, 2001). These corrections are used by rovers to calculate their precise coordinates.

The error between the reference station and rover is expressed as:

$$\Delta\delta\, D_{ij}^{k} = f(FKP_i^k, \Delta\varphi_{ij}, \Delta\lambda_{ij}, \Delta h_{ij}) \qquad (3.1)$$

This can be done separately from the network processing as only the rover coordinates and satellite information are necessary.

The dimensions of networks and the coverage of distribution media often make a linear FKP representation adequate. The coverage of a linear FKP model is then centered to a real reference station, and the FKP describe the horizontal gradients for the geometric and ionospheric signal components in the observation space (Figure 3.2).

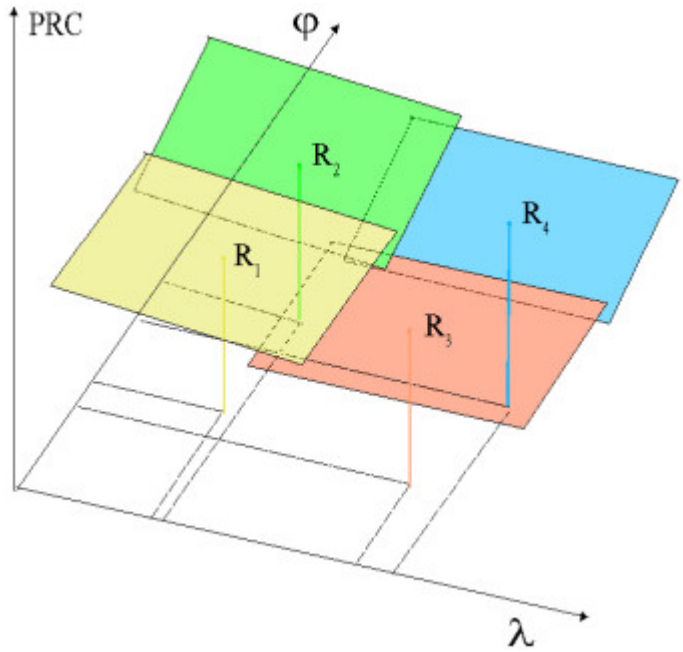

Figure 3.2. Linear FKP planes for four reference stations (Wubbena *et al*., 2001).

3.1.1.2. VRS Technique. The main idea of Virtual Reference Station (VRS) and VRS like solutions is that the corrections for rovers are transmitted as it is coming from the closest reference station. A Virtual Reference Station is generated by the networking program and the correction is transmitted over this essential station. This essential station is created in the same area with rover.

The rover does not understand that it is receiving a network correction and receives the correction as it is coming from a single reference station. So previous to the calculation of the corrections the rover has to send its first position to the server in NMEA data format.

The server generates VRS corrections particular for that rover. RTCM2.3 correction message with message type 59, which is incorporated inside is transmitted to the rover. RTCM is a format of standard corrections however for VRS only the transmitting data is standard not the content of the correction. Similar solutions have been published by different system providers as the VRS is a registered format (Lin, 2005, Landau *et al*., 2003, Wanninger *et al*., 2006).

In the event of Virtual Reference Stations (VRS) technique, it is needed to have two way communication between the Control Center and rovers. After the rover send its positions to Control Center, the center computes VRS reference data using all the CORS stations (Wubbena *et al*., 2001; Wanninger L., 1999; Vollath *et al*., 2000, 2001).

$$\overline{X}_{\mathrm{VRS}} = \overline{X}_{\mathrm{j}} \tag{3.2}$$

$$\mathrm{VRS}_{\mathrm{ij}}^{\mathrm{k}} = \mathrm{CPR}_{\mathrm{ij}}^{\mathrm{k}} + f(\mathrm{FKP}_{\mathrm{i}}^{\mathrm{k}}, \Delta\varphi_{\mathrm{ij}}, \Delta\lambda_{\mathrm{ij}}, \Delta h_{\mathrm{ij}}) + \Delta \mathrm{T}_{\mathrm{model,ij}} \tag{3.3}$$

Equation contains a tropospheric term $\Delta \mathrm{T}_{\mathrm{model,ij}}$, which defines the difference between the tropospheric delay model used in the network processing on the original reference station and the virtual reference station (Wubbena *et al*., 2001).

3.1.1.3. MAC Technique. Master Auxiliary Concept (MAC) is the basis of Real Time Correction Message (RTCM) 3.x net format. The corrections belonging to a sub-set, one master and several secondary stations, in the neighborhood of rovers are sent to rovers and precise coordinates calculated by the rover using these corrections.

In order to be able to utilize the data, RTK rover receivers have to be RTCM V3.0 coherent. They have to comprehend the RTCM V3.0 format and they have to be able to apply the network correction parameters. The RTK rovers receive RTCM V3.0 network data and the network correction parameters. RTCM3.0 data contains all of the required information for the entire network. A rover should be capable of understanding and applying these parameters.

The processes inside the MAC concept are described by RTCM. This provides transparency of the software that creates corrections for the field users. No need for any additional proprietary message. It is the Rover who decides ambiguity and computes precise position with the information receiver from networking software. This means the quality of the Rover coordinates are independent from the networking software as all the software working in RTCM 3.X format transmit the same type of data. So, different type of Rover providers can read the same data. As it is a unequalled correction parameter for all users only one way of correction transmission is required. One way channels like radio links can be used to transmit MAC network data and corrections. Besides, if the internet connection or GPRS connection is used only one way connection is required to transmit data (Brown *et al*., 2006).

3.1.2. CORS and GNSS-RTK Principles and Comparision

Network CORS solution has important benefits over classical GNSS positioning as listed below:

- Solutions up to 50 – 60 km baseline lengths from CORS stations, plus in shorter time,
- Automated solution in national ITRF_ coordinate systems,
- Elimination of systematic errors,
    - Up to 1 m in classical techniques
    - CORS approach < 1 cm + 1 ppm

- Much shorter field observation times,
- Real Time Kinematic (RTK) surveys in longer baselines (also more reliable),
    - Standard RTK < 5 - 10 km
    - CORS RTK < ~50 – 60 km.

The advantages of the CORS approach versus classical approach can be illustrated by an example in European side of Turkey (Figure 3.3.). In case of classical approach, Real Time Kinematik (RTK) ranges are 5 km, 7.5 km and 10 km corresponding to good, medium and poor solutions respectively. In case of CORS approach, RTK ranges are 40, 50 and 60 km corresponding to good, medium and poor solutions respectively. Besides, classical RTK coverage is about 150 km^2 whereas, CORS RTK coverage is 9600 km^2, 64 times larger than classical coverage.

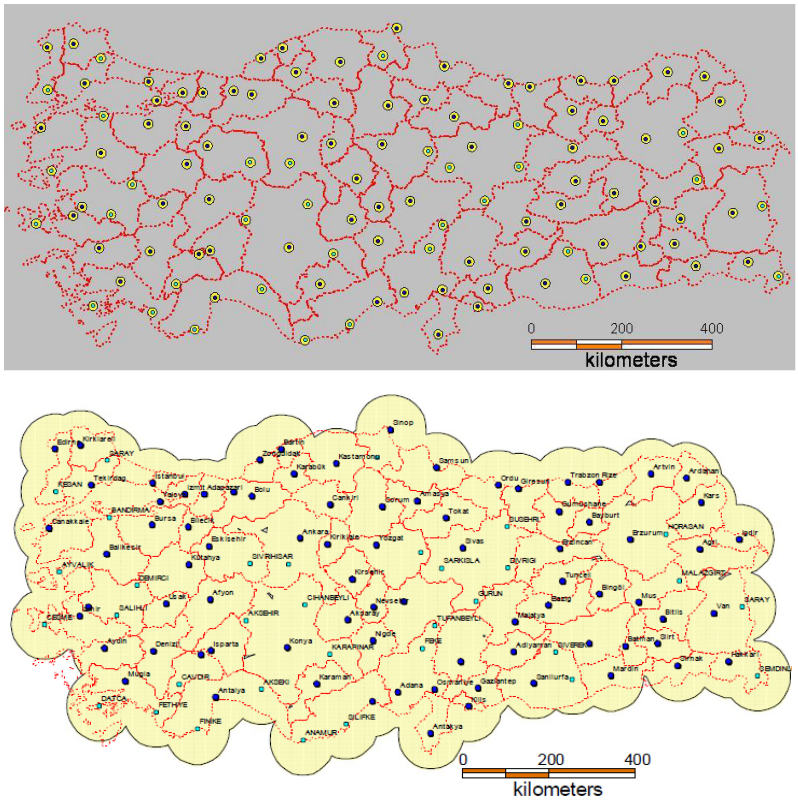

Figure 3.3. Classical and CORS Approach (Eren *et al*., 2009).

3.1.3. Benchmark Test

A performance benchmark test gives a repeatable set of measurable results from which present and future releases for specific functionality can be faithfully compared or baselined against. It means the similar test can be carried out again and again and a predictable set of metrics are produced.

The major objectives of the Benchmark (BM) test,

- Optimize the CORS network design,
- To test GNSS receivers and antenna,
- Evaluate Control Center software packages,
- To determine the most optimum interstation distances between CORS.

Three network configurations were chosen, each consisting of six CORS points: NET-120, NET-90 and NET-60 each one containing interstation distances of 120, 90 and 60 km respectively (Eren *et al*., 2009).

Table 3.1. CORS Network Distance (Eren *et al*., 2007).

NET-120	**NET-90**	**NET-60**	**Distance İnformation**
67	49	27	Min. Distance(km)
159	147	69	Max. Distance(km)
112	82	55	Mean Distance(km)
117	88	56	Rms. Distance(km)

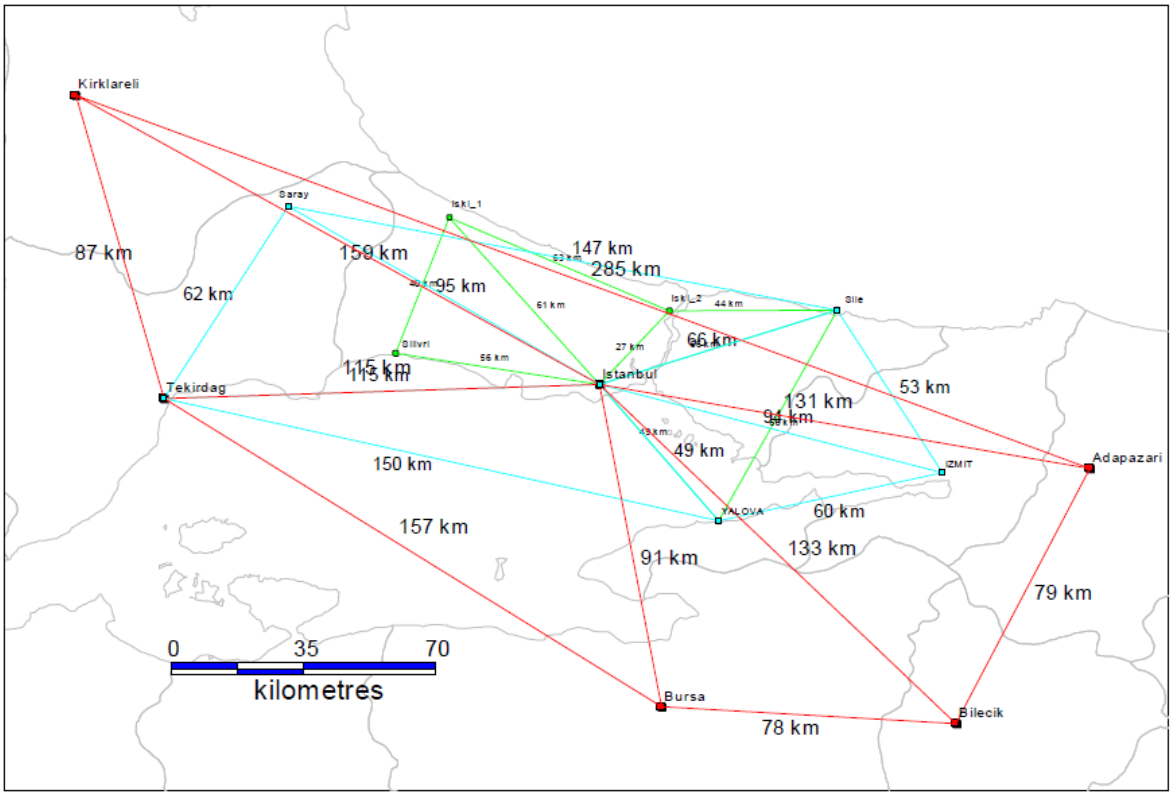

Figure 3.4. Benchmark test networks (Net-120, Net-90 and Net-60) (Eren *et al*., 2007).

Result of Benchmark test; CORS is also possible to use static surveys and determine precise coordinates in long baselines in minutes rather than hours in case of classical techniques (Eren *et al*., 2009).

3.2. GNSS CORS-TR System

General Directorate of Land Registry and Cadastre (GDLRC) in association with İstanbul Kültür University (IKU) and General Command of Mapping (GCM) offered the foundation of national continuously operating reference station (CORS) system that aimed,

- to establish network-based CORS-TR stations functioning 24 hours/day with RTK capabilities,

- to model the atmosphere (troposphere and ionosphere) over Turkey contributing to atmospheric studies and weather predictions and signal and communication studies,

- to provide mm-level accuracy for tracking plate tectonics, measuring deformations and contributing to earthquake prediction and early warning systems, to determine datum transformation parameters between the old system ED50 (European Datum-1950) and ITRF_ (International Terrestrial Reference Frame) (Kempe *et al*., 2006).

The proposal was sponsored by Scientific and Technological Research Council of Turkey (TUBITAK) on May 2006 and named as CORS-TR (or TUSAGA-AKTIF in Turkish). Based on the experiences and the results of the company performances, the final design of the CORS system (150 reference stations, three control centers, data communication systems) was prepared, 147 of 150 reference stations and 3 Control Centers (CC) were successfully established in Turkey and in Cyprus before the end of April 2009. The reference stations and the control centers have been in use since September 2009 (Figure 3.5).

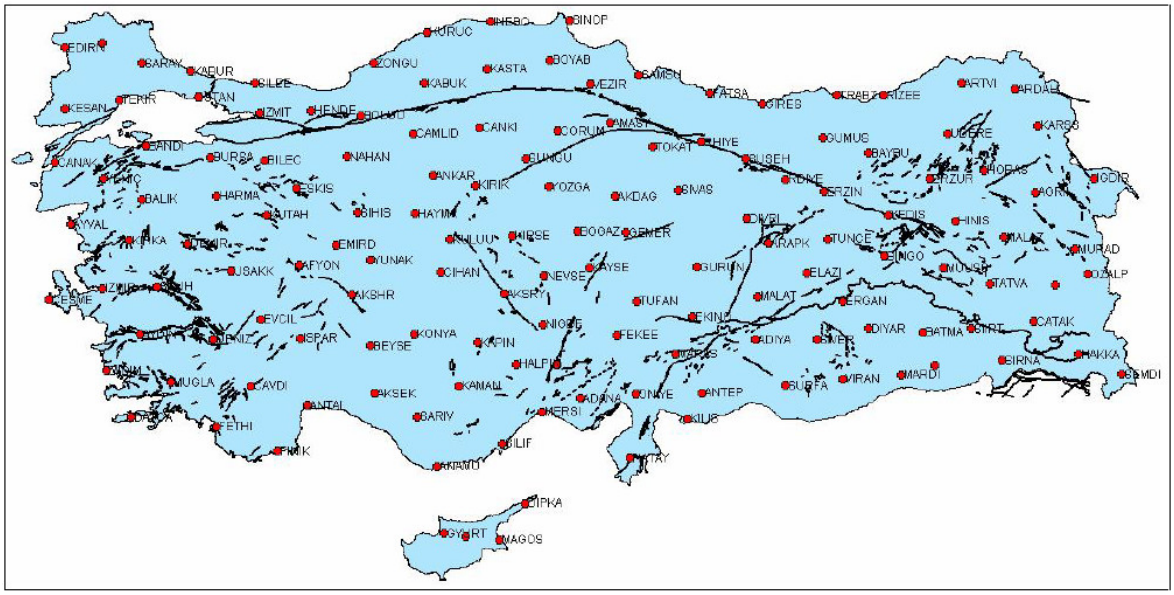

Figure 3.5. CORS-TR reference stations and main faults in Turkey and Cyprus.

3.2.1. CORS-TR Design

The implementation of a Continuously Operating GNSS Reference Station system is different for Real Time Kinematic (RTK) based applications, structural monitoring applications and crustal monitoring applications despite the fact the general content remains the same. In this section the equipments that are used for all type of CORS systems are described without any classification.

There are three main parts in CORS systems which are sites, control centers and users. The users are only relates with the results of the system. Another classification can be done for the processes in a CORS system as follows:

- Collection of the GNSS data at sites,
- Transmission of the CORS data to the Server,
- Production of Correction and File products,
- Transmission of the final products to the end user.

Technical visits and Benchmark Test (BM), CORS-TR was designed and the specifications of CORS systems were prepared according to wide research. The main features of the design consists of:

- Solid and practical pillars as monuments,
- Interstation distances of CORS were decided as 80 – 100 km,
- Dual-frequency GNSS receivers (GPS, GLONASS and GALILEO) with precise geodetic antenna,
- Two powerful Control Center (CC) and link to CC via ADSL and EDGE,
- Broadcasting of corrections of VRS, FKP and MAC by RTCM 3.0 and higher with the principle of NTRIP (Network Transport of RTCM through Internet Protocol) (Figure 3.6).

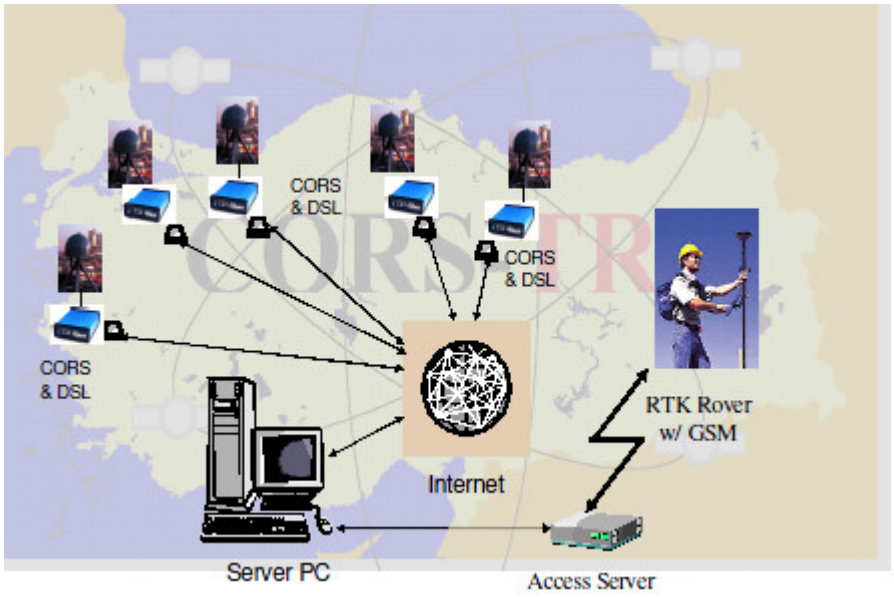

Figure 3.6. CORS-TR System Design.

3.2.2. CORS-TR Establishment

The type of monumentation of all 147 reference stations are decided upon ground and regional conditions. Concrete pillar are chosen for rigid ground stations while galvanized steel pillars are constructed for roof tops and roof terraces.

However, the heights of pillar change in terms of their positions. 86 of them are two meters tall concrete pillar, including ground pillars while 58 pillars on roof terraces are three meters and only three of them on roof tops is four meters galvanized steel pillars (Figure 3.7).

Figure 3.7. Antenna Types used in CORS-TR Reference Stations (two, three and four meters steel pillars).

3.2.3. Control Center

All the data from CORS-TR reference stations are automatically sent via internet to these control centers in which the network computations and positioning corrections are carried out and send sent to the users in the field. Control centers have a robust central software as well as servers (Figure 3.8). This software carries out these functions:

- Connecting all reference stations and transferring observations,
- Computing coordinates of reference stations,
- Modeling errors, computing corrections and broadcasting to rover stations (users),
- RTK services,
- Web services,
- Monitoring rovers,
- Storing all the data.

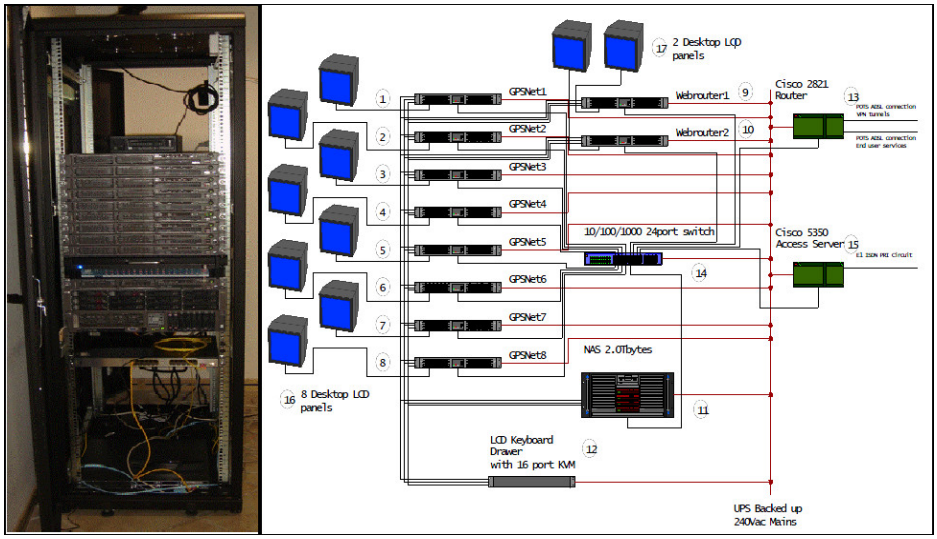

Figure 3.8. Master Control Station and its schematic representation.

The Master and Auxiliary Control Centers broadcast the coordinate correction using VRS CMR+, VRS RTCM 3.1, SAPOS FKP 2.3, RTCM3Net (MAC) and Differential Global Positioning System (DGPS) techniques. A separate webrouter transfers all the data from the reference stations to the main GPS net servers and auxiliary webrouter in real time (Figure 3.9).

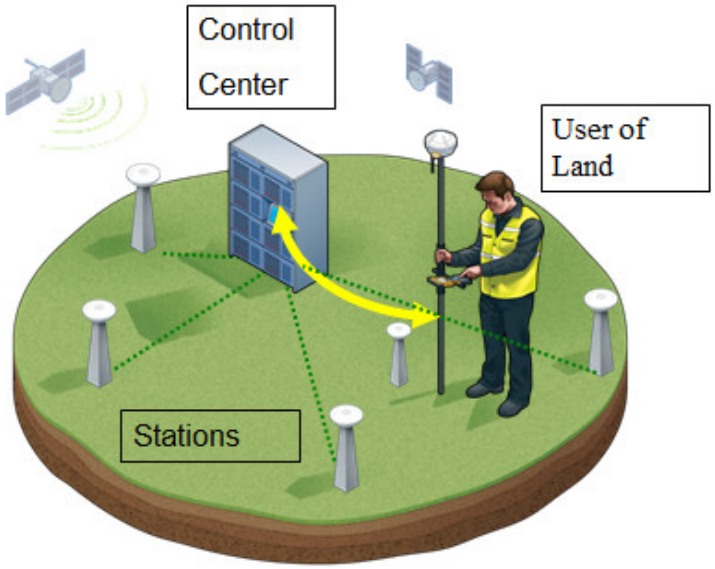

Figure 3.9. Use of CORS-TR VRS.

3.2.4. Central Processing Systems

Central Processing Concept covers the idea that all the raw data is collected by a Control Center Server Program and provides baseline solutions with near real time processing. The main vital of this system is that the system is designed with multi GNSS control points. However in RTK based system it is a responsibility to provide a RTK correction over a single GNSS receiver. It is remind that Network RTK corrections are used, the accuracy of network RTK systems for critical monitoring application is reasonable. With Central Processing all data is logged by the computer and using baseline solutions multiple calculations is executed to find the best result checks.

Most of the time, the distance between the monitoring sites are not too much. This provides better modeling in GPS applications. As the system is continuous system than generally single frequency (Only L1) receivers are enough for sufficient information associated with the site activity. Monitoring with dual-frequency GPS receivers relatively cost more and this evaluate the number of stations in the network (Brown *et al*., 2006).

High data sampling rates (more than 10 Hz) capacity of new GPS sensors provides the availability of slowly moving structural deformation detection (Ogaja *et al*., 2001a). Simultaneous computation of 3-D millimeter level accuracy positions are convenient with new age software programs which use both single and double frequency receivers together (Ogaja, 2002, Brown, 2006). In this system the raw data is processes in a centralized computer instead of in the rover monitoring GNSS receiver. Triple and double differenced data are processed to provide epoch-by-epoch Kalman-filtered solutions (Ogaja, 2002).

Single frequency monitoring with quasi-static initialization designed for single frequency monitoring. Quasi-static approach assumes lower dynamics as it is in most monitoring applications (Brown, 2006). L1 receivers are cheaper and more energy efficient and also do not require proprietary algorithms to extract high-quality measurements from the encrypted code on the L2 frequency. The disadvantage of single frequency receivers is that much less measurement data is available to help resolve the carrier phase ambiguities and to model the ionosphere. Also, many lower cost single frequency receivers have poor multipath mitigation capabilities (Brown, 2006).

3.2.5. Reference Stations

A total of 147 the CORS-TR reference stations are established in the field with baseline separation of 80-100 km as deduced from the prototype test (Figure 3.10). For every reference station, a GPS cabinet is specially designed for CORS-TR project. These cabinets have glass doors when used indoors or steel doors on outside use. They are designed to work independent of from city electricity network and feed on 12 Volt DC batteries.

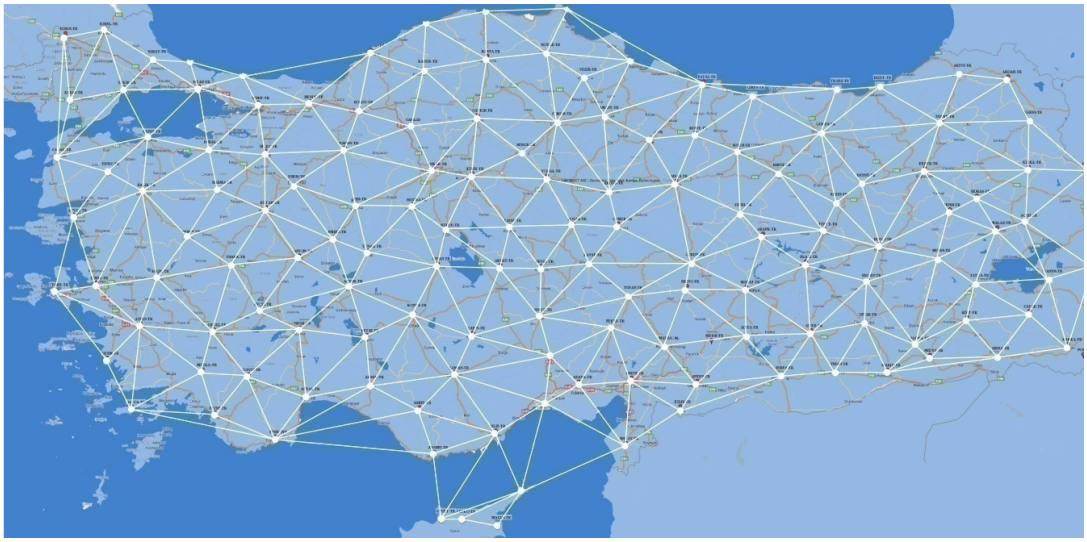

Figure 3.10. The network of CORS-TR stations.

3.2.6. CORS-TR Positioning Users

CORS-TR Project have very important contributions in the fields of civil applications. Some of these contributions are listed below:

- Geodetic measurements,
- Map measurements and Geographic Information Service (GIS),
- Planning and environmental studies,
- Monitoring of engineering structures,
- Monitoring of dams,
- Precise navigation and vehicle tracking,
- Infrastructure measurements and project applications,
- E-government, e-municipality, e-commerce applications, and
- All other geo-information projects.

CORS-TR system will be used in projects of planning, infrastructure, municipality, vehicle tracking, agriculture, forestry, cadastre, Geographic Information Service (GIS). This system will be highly beneficial for measuring Ground Control Points necessary for the operations of photogrammetric map production, ortho-rectification, ortho-photo production and other applications (Figure 3.11).

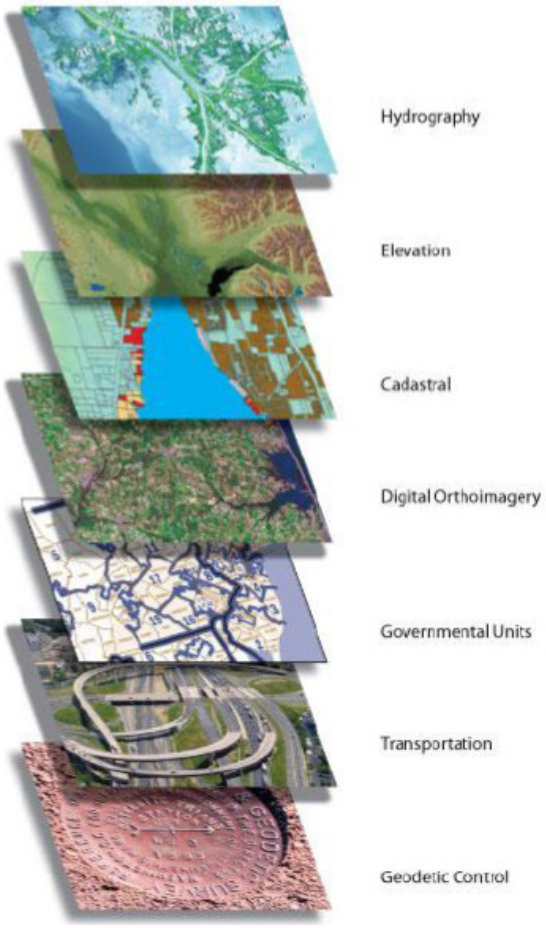

Figure 3.11. CORS-TR Applications.

3.2.7. CORS-TR Scientific Users

CORS-TR Project have very important contributions in the fields of scientific applications. Some of these contributions are listed below:

- Earthquake engineering,
- Seismology,
- Monitoring and analysis of disturbances in ionosphere and troposphere,
- Meteorology, and
- Smart transportation.

Horizontal Velocity field in a Eurasia-Fixed Frame using residual velocities of 17 IGS sites in Eurasia (ellipses are at 95% confidence level) as given Figure 3.12. (Aktuğ *et al*., 2009).

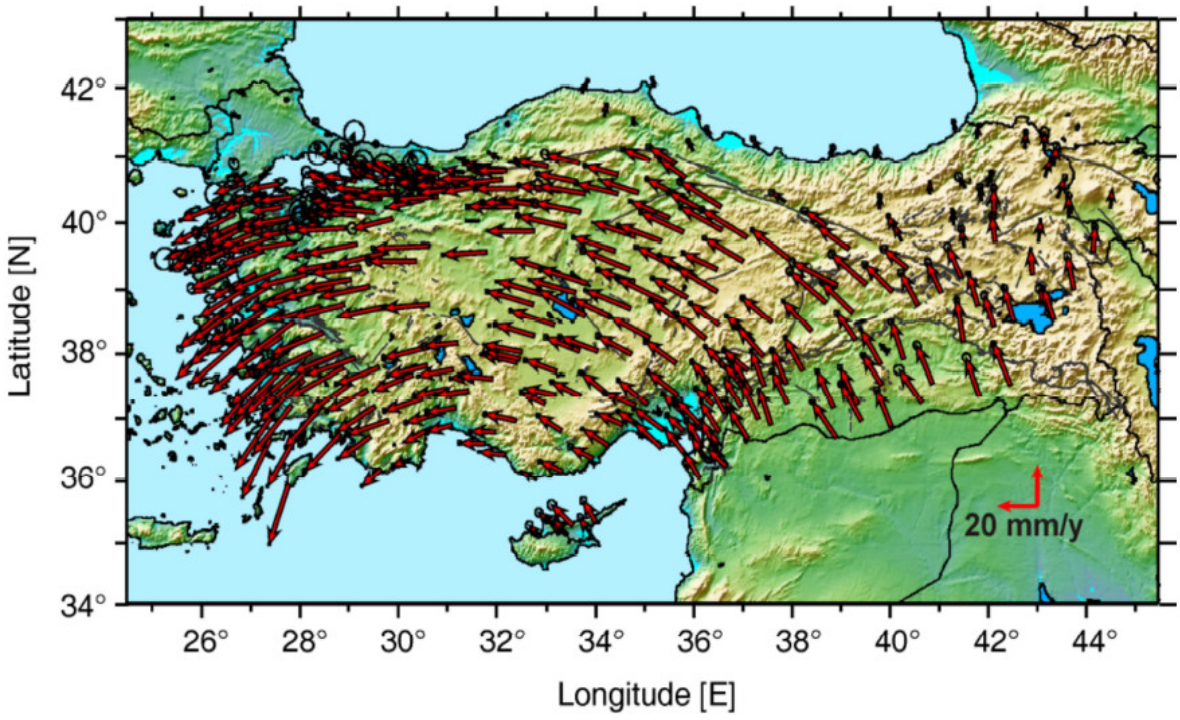

Figure 3.12. Velocity vectors with respect to Eurasian plate.

3.3. Data Used in Case Study

Tectonic movements in this area is a challenging task for diverse reasons and a devoted geodetic network for geodynamic objectives was constructed (Özener *et al.*, 2010). CORS-TR stations are established on the ground and on the roof of large but low-story governmental buildings (cadastre offices, meteorological observation stations, universities etc.) from where the technical support can be supplied. The distances between the stations range from 80-100 km (Figure 3.13).

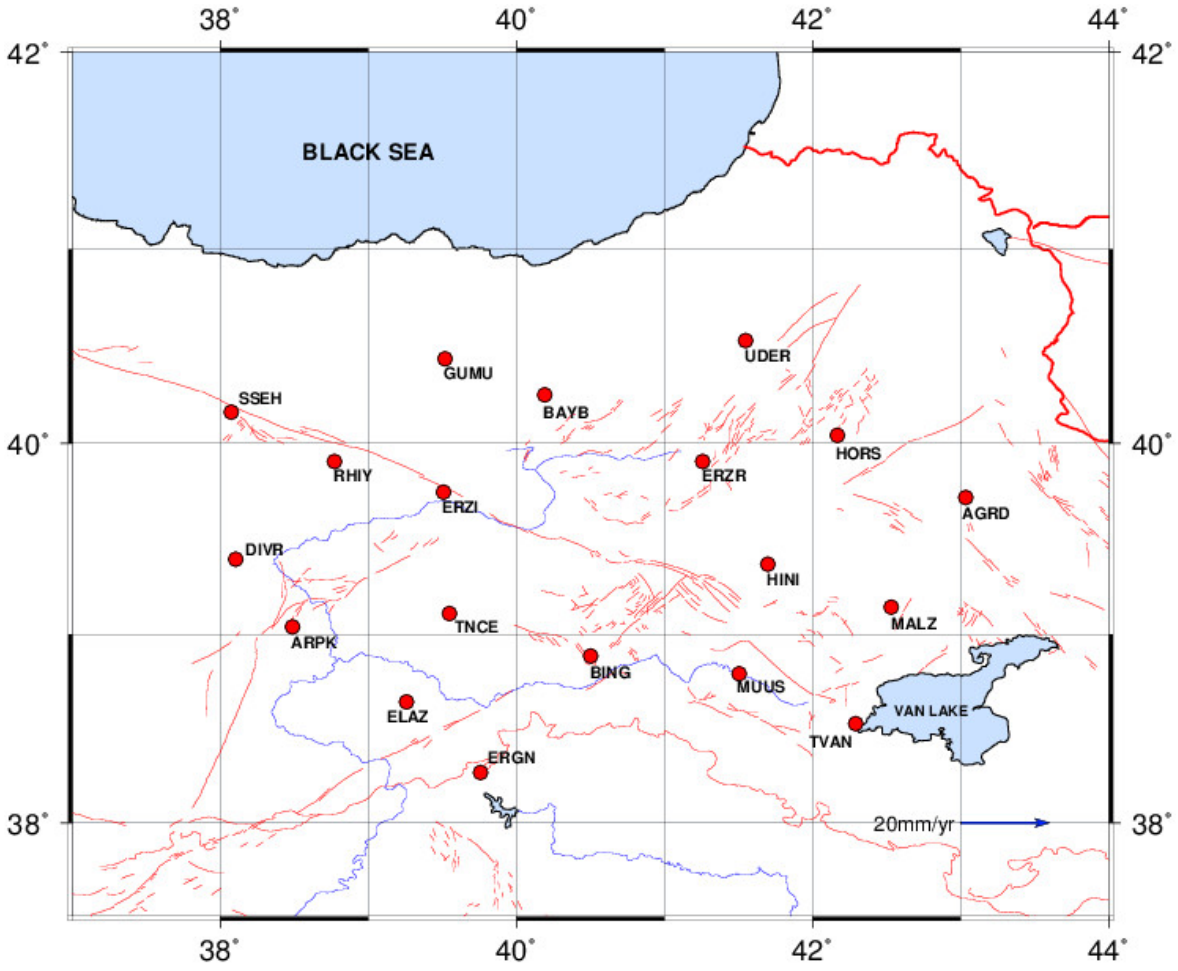

Figure 3.13. CORS-TR Stations in Study Area.

All CORS-TR reference stations are named in accordance with IGS regulations having only four characters. The coordinates and names of the CORS-TR reference stations are given in Table 3.2.

Data from nineteen CORS-TR refence stations have been used in this study. Six epochs of data from 2009 to 2012 were obtained for each stations.

Table 3.2. Coordinates of CORS-TR reference stations used fully study.

Station	**Station ID**	**Latitude (deg) WGS - 84**	**Longitude (deg) WGS - 84**
Ağrı	AGRD	39.71756	43.03287
Arapkir	ARPK	39.04059	38.48732
Bayburt	BAYB	40.25015	40.19144
Bingöl	BING	38.88545	40.50078
Divriği	DIVR	39.39432	38.10388
Elazığ	ELAZ	38.64467	39.25646
Ergani	ERGN	38.26961	39.75819
Erzincan	ERZI	39.74567	39.50607
Erzurum	ERZR	39.90561	41.25547
Gümüşhane	GUMU	40.43707	39.51617
Hınıs	HINI	39.36879	41.69579
Horasan	HORS	40.04165	42.16733
Malazgirt	MALZ	39.14316	42.53080
Muş	MUUS	38.79324	41.50216
Reşadiye	RHIY	39.90611	38.77080
Suşehri	SSEH	40.16247	38.07489
Tatvan	TVAN	39.52949	42.29046
Tunceli	TNCE	39.10697	39.54563
Uzundere	UDER	40.53128	41.54755

Table 3.3. CORS-TR reference stations dates and observation duration.

YEAR	Day of Year	Observation Duration	Data Rate (sec)
2009	084	24h	30
2009	268	24h	30
2010	084	24h	30
2011	115	24h	30
2011	329	24h	30
2012	116	24h	30

CORS-TR network equipped with Trimble NetR5 GNSS receivers, Permanent L1\L2, Compact L1\L2 and Zephyr Geodetic antennas, control centers provides RTK GPS positioning 24 hours a day (Figure 3.14).

Figure 3.14. Trimble NetR5 GNSS CORS receiver.

3.4. Selection of Software

3.4.1. GNSS CORS-TR Data Analyzing Software

In GNSS data processing, two types of software are used; commercial and scientific. Commercial software is used in common engineering applications and various types of GNSS data collected by any surveying method can be processed. Scientific software is generally used in crustal deformation studies but any kind of study which requires GNSS data processing can be carried out by scientific software. A list of scientific software and its supporting institution is given in Table 3.4.

Table 3.4. Scientific GNSS data processing software and supporting institutions.

Software	**Institute**
Bernese	AIUB
GAMIT/GLOBK	MIT-SIO
GIPSY/OASIS II	JPL (NASA)
PAGE5	NOAA
GEONAP	University of Hannover
MURO.COSM	University of Texas – Van Martin System
DIPOP	University of New Brunswick

GAMIT/GLOBK (Herring *et al*., 2010a) software is selected in this study for data process. The software works under two main modules. First module is GAMIT and it consists of various programs to process GNSS data and results return as the position estimates. The second main module is GLOBK which is a Kalman filter whose primary purpose is to combine various geodetic solutions from the processing of primary data from space geodetic or terrestrial observations.

The main GAMIT modules require seven types of input:

• Raw phase and pseudo-range data in the form of ASCII X-files (one for each station within each session)

• Station coordinates in the form of a L-file

• Receiver and antenna information for each site (file station.info)

• Satellite list and scenario (file session.info)

• Initial conditions for the satellites' orbits in a G-file (or a tabulated ephemeris in a T-file)

• Satellite and station clock values (I-, J-, and K-files)

• Control files for the analysis (sestbl. and sittbl.)

•"Standard" tables to provide lunar/solar ephemerides, the Earth's rotation, geodetic datums, and spacecraft and instrumentation information (Herring *et al*., 2010b).

GLOBK accepts as data, or "quasi-observations" the estimates and associated covariance matrices for station coordinates, earth-rotation parameters, orbital parameters, and source positions generated from analyses of the primary observations. These primary solutions should be performed with loose a priori uncertainties assigned to the global parameters, so that constraints can be applied uniformly in the combined solution. Although GLOBK has been developed as an interface with GAMIT (for GNSS) and CALC/SOLVE (for VLBI), there is little intrinsic to this pairing in its structure. GLOBK can be used to combine solution files generated by other GNSS software (*e.g.* Bernese and GIPSY), as well as for terrestrial and SLR observations.

There are three common modes, or applications, in which GLBOK is used:

1. Combination of individual sessions (*e.g.* days) of observations to obtain an estimate of station coordinates averaged over a multi-day experiment. For GPS analyses, orbital parameters can be treated as stochastic, allowing either short- or long-arc solutions.

2. Combination of experiment-averaged estimates of station coordinates obtained from several years of observations to estimate station velocities.

3. Independent estimation of coordinates from individual sessions or experiments to generate time series assessment of measurement precision over days (session combination) or years (experiment combination) (Herring *et al*., 2010c).

3.4.2. GNSS Data Analyzing Strategies

Data analyzing strategy is the first step to begin processing. Selection of the models and parameters are important as they have direct effect on the process results.

- Each campaign was processed using the International Terrestrial Reference Frame ITRF_.

- Precise final orbits by the International GNSS Service (IGS) were obtained in SP3 (Standard Product 3) format from SOPAC (Scripps Orbit and Permanent Array Center).

- Earth Rotation Parameters (ERP) came from USNO_bull_b (United States Naval Observatory_bulletin_b).

- 15 stations from IGS global monitoring network were included in the process. These IGS stations are TUBI, TRAB, ORID, ANKR, BUCU, ISTA, GRAZ, KIT3, MATE, NICO, NSSP, ONSA, SOFI, WTZR, ZECK.

- The 9-parameter Berne model was used for the effects of radiation and the pressure.

- Scherneck model was used for the solid earth tide and the ocean tide loading effects.

- Zenith Delay unknowns were computed based on the Saastamoinen a priori standard troposphere model with 2-h intervals.

- Iono-free LC (L3) linear combination of L1 and L2 carrier phases was used.

- The model, which depended on the height, was preferred for the phase centers of the antennas.
- Loosely constrained daily solutions obtained from GAMIT were included in the ITRF_ reference frame by a 7 parameters (3 offset–3 rotation–1 scale) transformation with 15 global IGS stations.

3.4.3. Kalman Filter

The Kalman Filter was designed to estimate the linear active systems (Kalman, 1960; Kalman and Bucy, 1961). According to Grewal and Andrews (1993), the Kalman Filter is an estimator for what is called the linear-quadratic Gaussian, while Maybeck (1979) claims that the Kalman Filter is simply an suitable recursive data processing algorithm.

The mathematical form of the Kalman Filter consists of two independent models, the active and measurement models given by the following formula (Kalman, 1960; Teunissen and Salzmann, 1988; Hofmann-Wellenhof *et al*., 1997; Leick, 1995):

$$x_k = \phi_{k,k-1}\, x_{k-1} + w_k \tag{3.4}$$

$$l_k = A_{k,k-1} + V_k \tag{3.5}$$

Where;

x_k is the state vector at time t_k

x_{k-1} is the state vector at time t_{k-1}

$\phi_{k,k-1}$ is the transition matrix from time t_{k-1} to t_k

w_k is the noise vector representing the dynamic model at time t_k

l_k is the observation vector at time t_k

A_k is the design matrix for the measurement model

V_k, is the noise vector, which represents the measurement model at time t_k.

Under the statistical assumptions described in Tsai and Kurz (1983) and Cross (1990), the prediction and filtering equations of the Kalman Filter can be summarized as follows. The prediction equations:

$$\bar{x}_k^- = \phi_{k,k-1}\ \bar{x}_{k-1} \tag{3.6}$$

$$Q_k^- = \phi_{k,k-1}\ Q_{k-1}\ \phi_{k,k-1}^T + Q_w \tag{3.7}$$

$$Q_w = \alpha^2_a\ w_k\ w^T_k \tag{3.8}$$

The filtering equations:

$$\bar{x}_k = \bar{x}_k^-\ K_k\ (l_k - A_k\ \bar{x}_k^-) \tag{3.9}$$

$$Q_k = (I - K_k\ A_k)\ Q_k^{-T} \tag{3.10}$$

$$K_k = Q_k^-\ A_k^T\ (A_k\ Q_k^-\ A_k^T + Q_l)^{-1} \tag{3.11}$$

Where;

$\bar{x}_k^-$ is the predicted estimate of the state vector at time t_k,

$\bar{x}_{k-1}$ is the filtered estimate of the state vector at time t_{k-1},

Q_k^- is the covariance matrix of the predicted state vector,

Q_w is the covariance matrix of the dynamic model noise,

σ_a^2 is the variance of the non-deterministic variable in the dynamic model,

Q_k is the covariance matrix of the filtered state vector,

K_k is the gain matrix.

Before deformation analysis can carried on, probable outliers should be detected. The most important criterion for the detection of outliers in Kalman Filters is the sequence (Salzmann, 1990):

$$v_k = l_k - A_k \bar{x}_k^- \tag{3.12}$$

Outliers can be detected by application of the local and global slippage tests (Teunissen and Salzmann, 1988). However, RT-MODS2 determines outliers only with the local slippage test because it is more suitable and simpler to implement for real-time applications than the global slippage test. Local slippage tests at time *tk*, depend only on the predicted state and the observations at time *tk* (Teunissen, 1990; Jin, 1996).

For an infinitely long, planar and vertical strike-slip fault locked from surface down to a depth of d (i.e., locking depth) the fault-parallel velocity (v) as a function of position (x) orthogonal to the fault is given by

$$V(x) = (v_p/\pi) - \tan^{-1}(x/d) \quad (3.13)$$

Where v_p is creeping rate of the deep fault below the locking depth (d) that is equal to the rate of plate velocity in the far field, and is often termed as slip rate, in which case it is assumed that crust is purely elastic and hence all the accumulated strain in the locked section of the fault is released coseismically.

3.5. CORS-TR Data Processing Results

CORS-TR reference stations data is processed by GAMIT/GLOBK software. Horizontal GPS velocities in Eurasia-fixed reference frame and plotted with 95 % confidence ellipses are shown in Figure 3.15. The velocities determined by using the data of six epochs between 2009 and 2012 are given in Table 3.5.

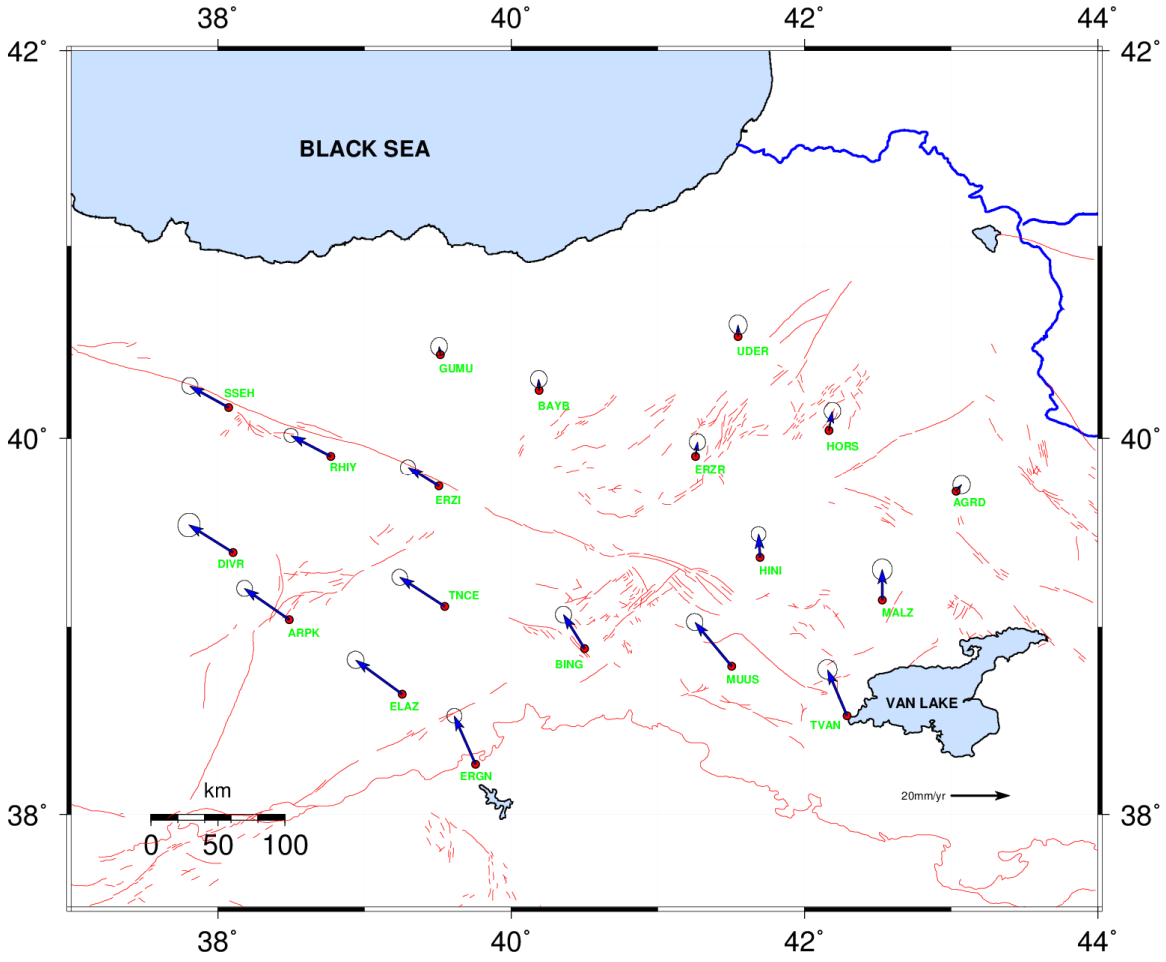

Figure 3.15. Horizontal GPS velocities in Eurasia-fixed frame and confidence ellipses plotted with 95 %.

Table 3.5. Summary of velocity estimates in Eurasia fixed reference frame.

Site	**Lon.** (°)	**Lat.** (°)	**V_e (mm/year)**	**V_n (mm/year)**	**σ_{Ve} (mm/year)**	**σ_{Vn} (mm/year)**	**ρ_{VeVn}**
AGRD	43.032	39.717	1.89	2.26	1.21	1.27	-0.001
ARPK	38.487	39.040	-15.30	10.60	1.10	1.11	-0.009
BAYB	40.191	40.250	-0.17	3.90	1.15	1.20	-0.000
BING	40.500	38.885	-7.22	11.60	1.14	1.16	-0.010
DIVR	38.103	39.394	-15.07	9.40	1.54	1.66	0.033
ELAZ	39.256	38.644	-15.89	11.60	1.17	1.20	-0.015
ERGN	39.758	38.269	-7.28	16.44	1.05	1.03	-0.013
ERZI	39.506	39.745	-10.52	6.54	1.05	1.07	-0.004
ERZR	41.255	39.905	0.70	4.89	1.14	1.16	-0.027
GUMU	39.516	40.437	-0.43	2.77	1.16	1.26	0.036
HINI	41.695	39.368	-0.49	7.95	1.04	1.03	-0.003
HORS	42.167	40.041	1.14	6.60	1.16	1.20	0.002
MALZ	42.530	39.143	-0.03	10.44	1.39	1.47	-0.011
MUUS	41.502	38.793	-12.56	14.99	1.16	1.18	-0.022
RHIY	38.770	39.906	-13.65	7.14	0.98	0.98	-0.011
SSEH	38.074	40.162	-13.30	7.33	1.12	1.16	-0.018
TVAN	42.290	38.529	-6.70	15.68	1.34	1.36	-0.027
TNCE	39.545	39.109	-15.32	9.93	1.08	1.11	-0.038
UDER	41.547	40.531	-0.00	4.04	1.25	1.36	-0.070

3.6. Combined Velocity Field

Following the estimation of velocities at 19 CORS-TR sites, the velocity fields produced by survey-mode measurements were combined at the velocity level (Aktuğ *et al*., 2009; Aktuğ *et al*., 2013). The velocity tables given in the literature provide the one sigma uncertainties and the correlation coefficient which is sufficient to construct a block covariance matrix for the combination. The velocities given in Aktuğ *et al*., (2013) and Reilinger *et al*., (2006) were transformed to the computed velocity field. Since the velocity table given in (Aktuğ *et al*., 2013) is already expressed in the same reference frame as (Reilinger *et al*., 2006), only one transformation was applied to transform both velocity tables to the one computed. The velocities to be combined in this study are those given in (Reilinger *et al*., 2006) and (Aktuğ *et al*., 2013). However, there are not any local common sites between these studies. Therefore, the common sites for the transformation were selected from IGS sites.

It was found that the combined velocity field of (Aktuğ *et al*., 2013) and (Reilinger *et al*., 2006) are in agreement with the CORS-TR velocity at 0.9930 mm/yr level. The common sites in both velocity fields and associated residuals are given Table 3.6**.**

Table 3.6. The common sites used in the transformation.

Site	Lon. (°)	Lat. (°)	V_e (mm/year)	V_n (mm/year)	r_e (mm/year)	r_n (mm/year)
ZECK-ZECK	41.5650	43.7880	1.88	2.54	0.8866	0.9651
ZELB-ZECK	41.5650	43.7880	1.88	2.54	0.8866	0.9651
WTZR-WTZR	12.8790	49.1440	1.37	0.29	0.9622	-0.6037
SOFI-SOFI	23.3950	42.5560	1.16	0.24	-0.0192	2.0435
ONSA-ONSA	11.9260	57.3950	-1.16	-0.49	0.1296	-1.0244
NSSP-NSSP	44.5030	40.2260	0.90	8.65	-2.0351	0.0184
NICO-NICO	33.3960	35.1410	-6.42	3.98	-0.3396	0.4925
MATE-MATE	16.7040	40.6490	0.99	4.76	-0.5358	-0.1592
KIT3-KIT3	66.8850	39.1350	0.13	0.96	-0.3484	-0.8338
GRAZ-GRAZ	15.4930	47.0670	0.89	0.82	0.0181	-0.1007
ITAY-ISTA	29.0200	41.1040	-0.40	-1.10	1.4667	-1.5516
BUCU-BUCU	26.1260	44.4640	0.15	-0.78	-0.7146	0.1803

Since, the field of study is much smaller than the distribution of the common points (IGS sites), any translations could be absorbed in the rotations. Therefore, estimating a simple Euler rotation matrix between the velocity fields was found to be sufficient. The transformation model used for the combination is:

$$v_2 = v_1 + R\,(\Omega \times r) \tag{3.14}$$

Where v_1, v_2 are the velocity vectors in both local frames, R is the transformation matrix from Cartesian to local coordinate system, and Ω is the Euler rotation vector and r is the position vector of each station. The estimated Euler Pole is given in Tables 3.7. and 3.8.

Table 3.7. Estimated Euler Pole in geographic units.

Lon. (°)	**Lat.** (°)	**Ω** (°/Ma)
-7.2156	-84.6516	0.0000000006

Table 3.8. Estimated Euler Pole in angular vector units.

X (mas/Myr)	**Y** (mas/Myr)	**Z** (mas/Myr)
-0.0002026	0.0021640	-0.0002752

The combined velocity field is tabulated in Table 3.12. The geographic distribution of three velocity fields is shown in Figure 3.16.

Table 3.9. The CORS-TR velocities.

Site	**Lon.** (°)	**Lat.** (°)	**V_e** **(mm/year)**	**V_n** **(mm/year)**	**σ_{Ve}** **(mm/year)**	**σ_{Vn}** **(mm/year)**	**ρ_{VeVn}**
AGRD	43.032	39.717	1.89	2.26	1.21	1.27	-0.001
ARPK	38.487	39.040	-15.30	10.60	1.10	1.11	-0.009
BAYB	40.191	40.250	-0.17	3.90	1.15	1.20	-0.000
BING	40.500	38.885	-7.22	11.60	1.14	1.16	-0.010
DIVR	38.103	39.394	-15.07	9.40	1.54	1.66	0.033
ELAZ	39.256	38.644	-15.89	11.60	1.17	1.20	-0.015
ERGN	39.758	38.269	-7.28	16.44	1.05	1.03	-0.013
ERZI	39.506	39.745	-10.52	6.54	1.05	1.07	-0.004
ERZR	41.255	39.905	0.70	4.89	1.14	1.16	-0.027
GUMU	39.516	40.437	-0.43	2.77	1.16	1.26	0.036
HINI	41.695	39.368	-0.49	7.95	1.04	1.03	-0.003
HORS	42.167	40.041	1.14	6.60	1.16	1.20	0.002
MALZ	42.530	39.143	-0.03	10.44	1.39	1.47	-0.011
MUUS	41.502	38.793	-12.56	14.99	1.16	1.18	-0.022
RHIY	38.770	39.906	-13.65	7.14	0.98	0.98	-0.011
SSEH	38.074	40.162	-13.30	7.33	1.12	1.16	-0.018
TVAN	42.290	38.529	-6.70	15.68	1.34	1.36	-0.027
TNCE	39.545	39.109	-15.32	9.93	1.08	1.11	-0.038
UDER	41.547	40.531	-0.00	4.04	1.25	1.36	-0.070

Table 3.10. The velocities given in Aktuğ *et al*., (2013).

Site	**Lon.** (°)	**Lat.** (°)	**V_e** **(mm/year)**	**V_n** **(mm/year)**	**σ_{Ve}** **(mm/year)**	**σ_{Vn}** **(mm/year)**	**ρ_{VeVn}**
SOLH	41.057	38.959	-10.18	15.00	0.66	0.64	-0.075
KRPR	40.733	39.182	-16.56	5.17	1.67	2.13	-0.062
GENC	40.575	38.758	-5.82	17.58	0.71	0.69	-0.131
ATAP	40.515	39.215	-18.85	5.79	1.62	2.13	-0.076
USVT	40.330	39.039	-21.06	8.35	1.96	2.58	-0.101
KLKY	40.105	38.949	-18.19	6.68	0.62	0.67	-0.043
KAKO	40.052	38.963	-18.19	6.68	0.62	0.67	-0.043
BLYM	40.038	39.430	-14.15	8.96	3.25	4.24	-0.053
KTAS	39.957	39.538	-13.60	3.34	1.52	1.88	-0.075
SRYB	39.910	38.737	-19.63	11.58	0.61	0.59	-0.072
KCMZ	39.524	39.824	-8.19	-0.93	1.18	1.47	-0.053
KLKT	39.420	40.151	-5.79	2.86	0.35	0.38	-0.034
SRTS	39.258	39.350	-20.10	4.59	1.28	1.59	-0.051
HZAT	39.217	39.074	-21.49	12.57	1.50	1.86	-0.069
CMGK	39.164	39.613	-15.64	9.20	0.40	0.51	-0.100
CMG1	38.931	39.026	-19.92	13.05	0.83	0.98	-0.089
DBAS	38.922	39.059	-19.92	13.05	0.83	0.98	-0.089
ILIC	38.645	39.310	-22.76	10.25	1.37	1.67	-0.085
DIVR	38.515	39.614	-20.88	11.27	0.41	0.49	-0.113

Table 3.11. The velocities given in Reilinger *et al*., (2006).

Site	**Lon.** (°)	**Lat.** (°)	**V_e (mm/year)**	**V_n (mm/year)**	**σ_{Ve} (mm/year)**	**σ_{Vn} (mm/year)**	**ρ_{VeVn}**
SINC	37.958	39.454	-17.03	10.01	0.44	0.43	0.001
GMKV	39.254	38.640	-13.64	10.88	1.24	1.20	-0.046
TUNC	39.524	39.071	-16.97	11.96	1.45	1.30	-0.004
KAKO	40.052	38.963	-13.53	9.87	1.58	1.36	-0.012
MERC	40.254	39.731	-2.81	5.81	0.75	0.68	-0.015
SOLH	41.057	38.959	-6.75	11.47	1.43	1.20	-0.024
ISPI	40.809	40.437	0.72	3.31	0.56	0.51	-0.015
ERZU	41.300	39.973	-0.66	5.88	0.66	0.64	0.008
VART	41.454	39.186	-5.88	10.74	2.01	1.29	-0.046
TKMN	41.512	39.643	-2.09	4.39	1.78	1.22	-0.072
KRKT	41.794	38.754	-4.69	14.76	0.84	0.69	0.107
OLTU	41.990	40.548	1.95	5.07	0.93	0.90	0.020
KRYZ	42.149	39.714	-1.42	8.81	1.40	1.24	-0.022
RESD	42.547	38.488	-5.62	14.01	1.52	1.20	-0.045
PTNS	42.910	39.232	-2.03	9.45	0.61	0.52	-0.032
ARGI	43.026	39.719	0.84	8.66	0.68	0.65	-0.036

Table 3.12. The combined velocities.

Site	**Lon.** (°)	**Lat.** (°)	$\mathbf{V_e}$ **(mm/year)**	$\mathbf{V_n}$ **(mm/year)**	$\boldsymbol{\sigma_{Ve}}$ **(mm/year)**	$\boldsymbol{\sigma_{Vn}}$ **(mm/year)**	$\boldsymbol{\rho_{VeVn}}$
SINC	37.958	39.454	-16.84	10.37	0.44	0.43	0.001
GMKV	39.254	38.640	-13.45	11.23	1.24	1.20	-0.046
TUNC	39.524	39.071	-16.78	12.31	1.45	1.30	-0.004
KAKO	40.052	38.963	-13.34	10.22	1.58	1.36	-0.012
MERC	40.254	39.731	-2.61	6.16	0.75	0.68	-0.015
SOLH	41.057	38.959	-6.55	11.81	1.43	1.20	-0.024
ISPI	40.809	40.437	0.92	3.66	0.56	0.51	-0.015
ERZU	41.300	39.973	-0.46	6.23	0.66	0.64	0.0080
VART	41.454	39.186	-5.68	11.09	2.01	1.29	-0.046
TKMN	41.512	39.643	-1.89	4.74	1.78	1.22	-0.072
KRKT	41.794	38.754	-4.49	15.10	0.84	0.69	0.1070
OLTU	41.990	40.548	2.16	5.41	0.93	0.90	0.0200
KRYZ	42.149	39.714	-1.22	9.15	1.40	1.24	-0.022
RESD	42.547	38.488	-5.42	14.35	1.52	1.20	-0.045
PTNS	42.910	39.232	-1.82	9.79	0.61	0.52	-0.032
ARGI	43.026	39.719	1.05	8.99	0.68	0.65	-0.036
SOLH	41.057	38.959	-9.98	15.35	0.66	0.64	-0.075
KRPR	40.733	39.182	-16.36	5.52	1.67	2.13	-0.062
GENC	40.575	38.758	-5.62	17.93	0.71	0.69	-0.131
ATAP	40.515	39.215	-18.65	6.14	1.62	2.13	-0.076
USVT	40.330	39.039	-20.86	8.70	1.96	2.58	-0.101
KLKY	40.105	38.949	-17.99	7.03	0.62	0.67	-0.043
KAKO	40.052	38.963	-17.99	7.03	0.62	0.67	-0.043
BLYM	40.038	39.430	-13.95	9.31	3.25	4.24	-0.053
KTAS	39.957	39.538	-13.40	3.69	1.52	1.88	-0.075
SRYB	39.910	38.737	-19.44	11.93	0.61	0.59	-0.072
KCMZ	39.524	39.824	-7.99	-0.58	1.18	1.47	-0.053
KLKT	39.420	40.151	-5.59	3.21	0.35	0.38	-0.034
SRTS	39.258	39.350	-19.90	4.94	1.28	1.59	-0.051
HZAT	39.217	39.074	-21.30	12.93	1.50	1.86	-0.069
CMGK	39.164	39.613	-15.45	9.56	0.40	0.51	-0.100
CMG1	38.931	39.026	-19.73	13.41	0.83	0.98	-0.089
DBAS	38.922	39.059	-19.73	13.41	0.83	0.98	-0.089
ILIC	38.645	39.310	-22.57	10.61	1.37	1.67	-0.085
DIVR	38.515	39.614	-20.69	11.63	0.41	0.49	-0.113

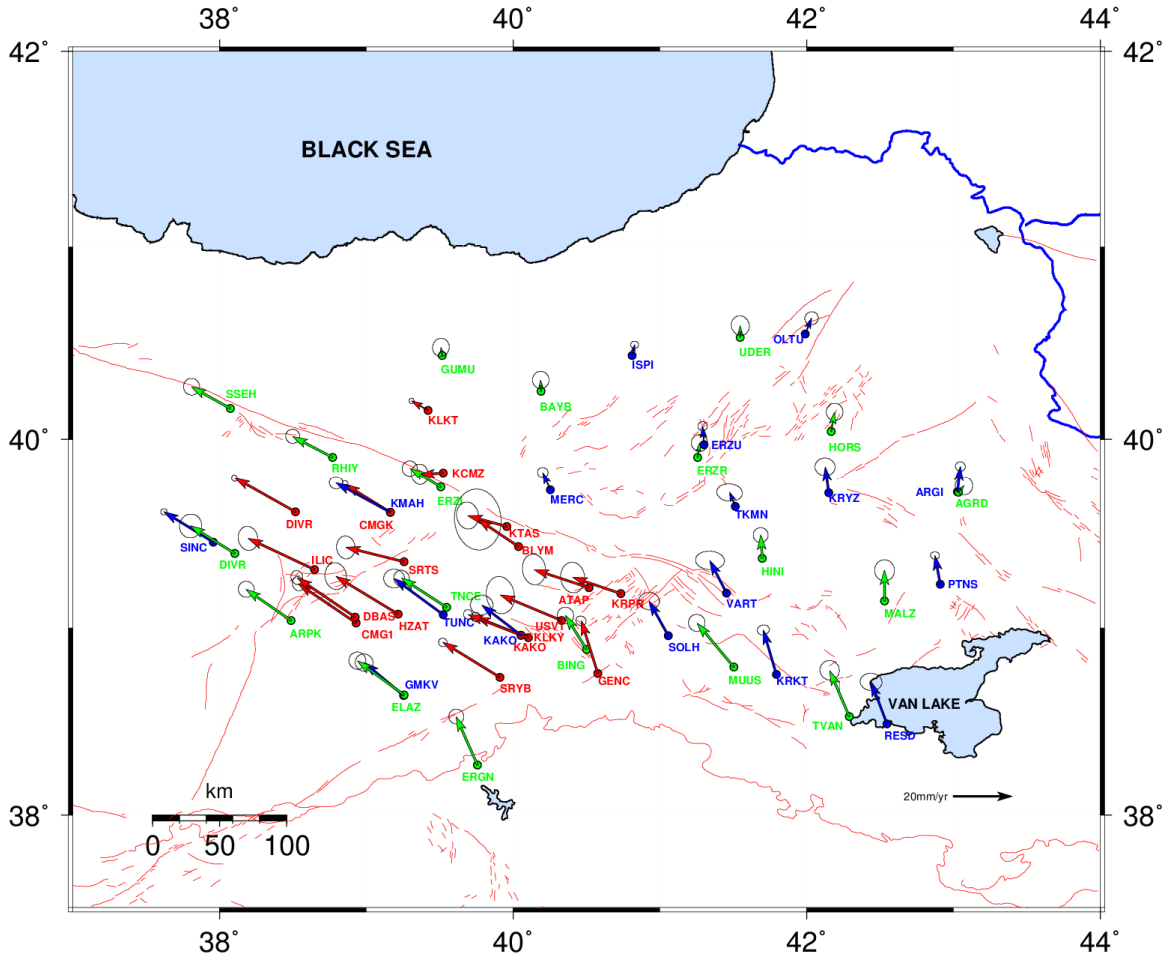

Figure 3.16. GPS velocities from Reilinger *et al*., (2006) in blue, Aktuğ *et al*., (2013) in red and CORS-TR in green.

4. RESULTS AND DISCUSSION

GPS measurements have been used for crustal deformation for many years. However, a reliable estimation of velocity field through GNSS requires a long span of data which can be collected by campaing type surveys or from continuous stations. The GNSS observation campaigns provide valuable information on the tectonic plate movements within a particular region.

CORS networks are useful tools as they collect data for 24 hours and can cover a wide area. The CORS network implemented in Turkey consists of 147 stations spread around the whole country and named as CORS-TR network.

In this study, 19 CORS-TR network stations which are located in eastern Turkey have were used to derive a velocity. Eastern Turkey is a seismically active and interesting place as three plates meet at Karlıova Triple Junction.

As explained in the result chapter, between 2009-2012 six epochs CORS-TR data obtained from the nationwide network the similar results with Reilinger *et al*., (2006) and Özener *et al*., (2010) studies. Figure 4.1. show the estimated velocities relative to a reference point located outside of the main deforming area in order to highlight the local velocities in the eastern part of Anatolia (Özener *et al*., 2010).

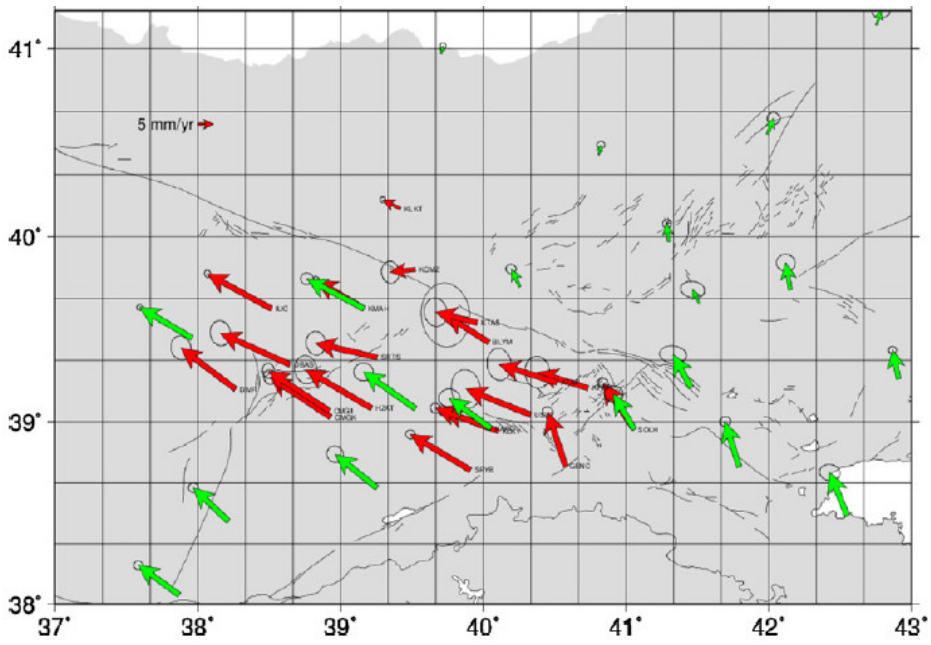

Figure 4.1. GPS velocities from Reilinger *et al*., (2006) in green and Özener *et al*., (2010) in red.

The eastern Anatolian contractional zone, consisting of a collage of oceanic and continental crust, is an active collisional convergent zone that is still being squeezed between the Arabian and Eurasian plates. This collisional zone is also identified as a compressional–extensional tectonic regime, driven by the westward extrusion of the Anatolian plate along the right-lateral NAFS and left-lateral EAFS (Şengör and Yılmaz, 1981).

Stations have northwest directed displacements relative to Eurasia, consistent with the right-lateral NAFZ. A further attempt was made to densify the computed velocity field. For this purpose, velocity field published in (Aktuğ *et al*., 2013) was trasformed into the velocity field computed through CORS network. Since, the velocity field given in (Aktuğ *et al*., 2013) has already been tranformed to the frame given in (Reilinger *et al*., 2006), a single transformation was applied to tranform both velocity fields given in (Aktuğ *et al*., 2013) and (Reilinger *et al*., 2006). The obtained precision for the transformation is below 1 mm/yr and is within the uncertainty level of the velocity field. The combined velocity fields provides the most dense velocity field in the region, available.

While CORS-TR network with its RTK capability has been installed with practical surveying purposes, it has been shown that it is still useful for crustal deformation to a certain extent. And even this network may be used in cooperation with the neighboring CORS-TR networks in order to give a better understanding in the characteristics of the Eurasian, African, Arabian plates and wider monitored regions rather than Anatolia.

This study focused on the idea of dealing with a crustal deformation monitoring project by using different geodetic techniques. Moreover, this study tried to form interactions between different disciplines of geosciences and geodesy in terms of deformation monitoring projects.

In conclusion, the results of this study and prior studies indicate that, the North Anatolian Fault and East Anatolian Fault and East Anatolian Fault are active faults and have the potential to create a catastrophic earthquake which would affect millions of people.

REFERENCES

Aktuğ, B., A. Kılıçoğlu, O. Lenk and M. A. Gürdal, 2009, "Establishment of Regional Reference Frames for Quantifying Active Deformation Areas in Anatolia", *Studia Geophysica et Geodaetica*, Vol. 53 (2), pp. 169-183.

Aktuğ, B., U. Dikmen, A. Doğru and H. Özener, 2013, "Seismicity and Strain Accumulation around Karlıova Triple Junction (Turkey)", *Journal of Geodynamics*, Vol.67, pp.21-29.

Ambraseys, N.N., 1970, "Some Characteristic Features of the North Anatolian Fault Zone", *Tectonophysics* Vol. 9, pp. 143-165.

Ambraseys, N.N., 1971, "Value of Historical Records of Earthquakes", *Nature* Vol. 232, pp. 375-379.

Ambraseys, N.N. and J. A. Jackson, 1998, "Faulting Associated with Historical and Recent Earthquakes in the Eastern Mediterranean Region", *Geophysical Journal International* Vol. 133, pp. 390-406.

Arpat, E. and F. Saroğlu, 1972, "The East Anatolian Fault System: Thoughts on its Development", *M.T.A. Bull.*, Vol. 78, pp. 33–39.

Avcı, O., 2007, *The Design and Use of the Continuous GNSS Reference Networks*, M.S. Thesis, Boğaziçi University, KOERI, Istanbul.

Barka, A. and K. Kadinsky-Cade, 1988, "Strike–Slip Fault Geometry in Turkey and Influence on Earthquake Activity", *Tectonics*, Vol.7, No.3 pp.663–684.

Bozkurt, E., 2001, "Neotectonics of Turkey—A Synthesis", *Geodinamica Acta* Vol. 14, pp. 3-30.

Brown, N., I. Geisler and L. Troyer, 2006, "RTK Rover Performance Using the Master-Auxiliary Concept", *Proceedings of Journal of Global Positioning Systems*, Vol. 5, pp. 135-144.

Brown, N., L. Troyer, O. Zelzer and J. Cranenbroek, 2006, "Advances in RTK and Post Processed Monitoring with Single Frequency GPS", *Proceedings of Journal of Global Positioning Systems*, Vol. 5, pp. 145-151.

Cross, P. A., 1992, "Advanced Least Squares Applied to Position Fixing", *Working Paper No. 6*, Department of Land Information, University of East London.

Dewey, J. F. and A. M. C. Şengör, 1979, "Aegean and Surrounding Region: Complex Multiplate and Continuum Tectonics in a Convergent Zone", *Geological Society of America Bulletin,* Vol. 90 (1), pp. 84–92.

Dewey, J. F., M. R. Hempton, W. S. F. Kidd, F. Saroğlu and A. M. C. Şengör, 1986, "Shortening of Continental Lithosphere: The Neotectonics of Eastern Anatolia-A Young Collision Zone, In Collision Tectonics", *Geological Society Special Publication* Vol. 19 pp. 3-36.

Doğru A., 2010, "Deformation of Eastern Turkey from Seismic and Geodetic Strain Rates", *Scientific Research and Essays*, Vol. 5 (9), pp. 911-916.

Emre, O. and T. Y. Duman, 2007, "The East Anatolian Fault: Structural Pattern and Relationship with the Dead Sea Transform", *Transactions American Geophysical Union*, 88(52), Fall Meeting Supplement., Abstract T42B-01.

Eren K., T. Uzel, E. Gülal, O. Yıldırım and A. Cingöz, 2009, "Results from a Comprehensive GNSS Test in the CORS-TR Network: Case Study", *Journal of Surveying Engineering*, USA.

Ergün, M., M. Aktar and H. Eyidoğan, 2004, "Present-day Seismicity and Seismotectonics of the Cilician Basin: Eastern Mediterranian Region of Turkey", *Bulletin of the Seismological Society of America* 94, 930-939.

Fontaine, J. M., O. Monod, J. Braud and D. Perinçek, 1989, "The Hezan Units: A Fragment of the South Neo-Tethyan Passive Continental Margin in South East Turkey", *Journal of Petroleum Geology 12*, pp. 29-50.

Grewal, M. S. and A. P. Andrews, 1993, "Kalman Filtering Theory and Practice", *Information and System Sciences Series*, pp.380, Englewood Cliffs, New Jersey.

Gürsoy, H., O. Tatar, J. D. A. Piper, A. Heimann and L. Mesci, 2003, "Neotectonic Deformation Linking the East Anatolian and Karatas-Osmaniye Intracontinental Transform Fault Zones in the Gulf of Iskenderun, Southern Turkey, Deduced from Palaeomagnetic Study of the Ceyhan-Osmaniye Volcanics", *Tectonics* 22.

Havazlı, E., 2012, *Determination of Strain Accumulation Along Tuzla Fault*, M.S. Thesis, Boğaziçi University, KOERI, Istanbul.

Hempton, M. R., J. F. Dewey and F. Saroğlu, 1981, "The East Anatolian Transform Fault: Along Strike Variations in Geometry and Behaviour", *Transactions American Geophysical Union*, Vol. 62, pp. 393.

Hempton, M. R., 1985, "Structure and Deformation History of the Bitlis Suture Near Lake Hazar, Southeastern Turkey", *Geological Society of American Bulletin* 96, pp. 233-243.

Hempton, M. R., 1987, "Constraints on Arabian Plate Motion and Extensional History of the Red Sea", *Tectonics*, Vol. 6, pp. 687–705.

Herece, E and E. Akay, 2003, "Kuzey Anadolu Fayı Atlası", *Maden Tetk. Arama Genel Müdürlüğü Özel Yayın*, pp. 13, Ankara.

Herring, T. A., R. W. King and S. C. McClusky, 2010a, "GAMIT Reference Manual GPS Analysis at MIT Release 10.3", *Department of Earth, Atmospheric, and Planetary Sciences* Massachussetts Institute of Technology.

Herring, T. A., R. W. King and S. C. McClusky, 2010b, "Introduction to GAMIT/GLOBK Release 10.3", *Department of Earth, Atmospheric, and Planetary Sciences* Massachusetts Institute of Technology.

Herring, T. A., R. W. King and S. C. McClusky, 2010c, "Global Kalman Filter VLBI and GPS Analysis Program", *Department of Earth, Atmospheric, and Planetary Sciences* Massachusetts Institute of Technology.

Hofmann-Wellenhof, B., H. Lichtenegger and J. Collins, 1997, "GPS: Theory and Practice", *Springer Verlag*, Vol. 4, pp. 370, New York.

Eren K., T. Uzel and E. Gülal, 2007, CORS-TR Benchmark Test Results, Istanbul Kultur University, http://cors-tr.iku.edu.tr/En_test_programi_genel.htm

Helland, V., 2005, Tectonics and Earthquakes, University of Wisconsin-Eau Claire, http://academic.evergreen.edu/g/grossmaz/HAMMVM/

Jackson, J. A. and D. McKenzie, 1988, "The Relationship between Plate Motions and Seismic Moment Tensors, and the Rates of Active Deformation in the Mediterranean and Middle East." *Geophys. J*, Vol. 93, pp. 45-73.

Jin, X., 1996, “Theory of Carrier Adjusted DGPS Positioning Approach and Some Experimental Results”, *Delft University Press*, pp. 164, Netherlands.

Kalman, R. E., 1960, “A New Approach to Linear Filtering and Prediction Problems”, *Journal of Basic Engineering*, pp. 35–45.

Kalman, R. E. and R. S. Bucy, 1961, “New Results in Linear Filtering and Prediction Theory”, *Journal of Basic Engineering*, pp. 95–108.

Kasapoğlu, K. E. and M. N. Toksöz, 1983, “Tectonic Consequences of the Collision of the Arabian and Eurasian Plates: Finite Element Models”, *Tectonophysics* Vol. 100, pp. 71–95.

Kempe, C., A. Alfredsson, L. E. Engberg and M. Lilje, 2006, "Correction Model to Rectify Distorted Coordinate Systems", *FIG Congress*, Munich, Germany.

Kiratzi, A. A. and C. B. Papazachos, 1995, “Active Crustal Deformation of North and East Anatolian Fault Zones”, *Tectonophysics* 243 pp. 1–24.

Koçyiğit, A. and A. Özaçar, 2003, “Extensional Neotectonic Regime through the NE Edge of the Outer Isparta Angle, SW Turkey”, *Turkish Journal of Earth Sciences*, Vol. 12, pp. 67-90.

Kozacı, O., J. F. Dolan, R. Finkel and R. Hartleb, 2007, “Late Holocene Slip Rate for the North Anatolian Fault, Turkey, from Cosmogenic 36Cl Geochronology: Implications for the Constancy of Fault Loading and Strain Release Rates.” *Geology* Vol. 35, pp. 867–870.

Landau, H., U. Vollath and X. Chen, 2003, “Virtual Reference Stations versus Broadcast Solutions in Network RTK-Advantages and Limitations”, *In Proceedings of GNSS*, Graz, Austria.

Leick, A., 1995, "GPS Satellite Surveying", *John Wiley and Sons*, pp. 584.

Le Pichon, X., F. Bergerat and M. J. Roulet, 1988, "Plate Kinematics and Tectonics Leading to the Alpine Belt Formation: A New Analysis", *Geological Society of America*, Vol. 218, pp. 111 – 131.

Lin, M., 2005, "RTCM 3.0 Implementation South Alberta Network", *ION GNSS 18th International Technical Meeting of the Satellite Division,* Long Beach, California.

Maybeck, P. S., 1979, "Stochastic Models", *Academic Press*, Vol. 1, pp. 423, New York.

McKenzie, D.P., 1970, "Plate tectonics of the Mediterranean Region", *Nature*, 226, pp. 239-243.

McKenzie, D., 1972, "Active tectonics of the Mediterranean Region", *Geophysical Journal of the Royal Astronomical Society*", Vol. 30, pp. 109–185.

McKenzie, D., 1976, "The East Anatolian Fault: A major Structure in Eastern Turkey", *Earth Planet Science*, Vol. 29, pp. 189– 193.

McClusky, S., S. Balassania, A. Barka, C. Demir, S. Ergintav, I. Georgiev, O. Gürkan, M. Hamburger, K. Hurst, H. Kahle, L. Kastens, G. Kekelidze, R. W. King, V. Kotzev, O. Lenk, S. Mahmoud, A. Mishin, M. Nadariya, A. Ouzounis, D. Paradissis, Y. Peter, M. Prilepin, R. Reilinger, I. Şanlı, H. Seeger, A. Taeleb, M. N. Toksoz and G. Veis, 2000, "GPS Constraints on Plate Motions and Deformation in the Eastern Mediterranean: Implications for Plate Dynamics", *Journal of Geophysical Research*, V. B105, No. B3, pp. 5695-5719.

Meade, B. J., B. H. Hager, S. C. McClusky, R. E. Reilinger, S. Ergintav, O. Lenk, A. Barka and H. Özener, 2002, "Estimates of seismic potential in the Marmara Sea region from block models of secular deformation constrained by Global Positioning System measurements", *Bulletin of the Seismological Society of America*, Vol. 92, and pp. 208–215.

Meghraoui, M., Z. Çakır, F. Masson, Y. Mahmoud, S. Ergintav, A. Alchalbi, S. İnan, M. Daoud, Ö. Yönlü and E. Altunel, 2011, "Kinematic Modelling at the Triple Junction between the Anatolian, Arabian, African plates (NW Syria and in SE Turkey)", *Geo-physical Research Abstracts*, Vol. 13, EGU2011-12599, EGU General Assembly, Vienna.

Nalbant, S. S., J. McCloskey, S. Steacy and A. A. Barka, 2002. "Stress Accumulation and Increased Seismic Risk in Eastern Turkey", *Earth and Planetary Science Letters* Vol. 195, pp. 291-298.

Ogaja, C., C. Rizos and J. Wang, 2001a, "Toward the Implementation of On-Line Structural Monitoring Using RTK-GPS and Analysis of Results Using the Wavelet Transform", *FIG International Symposium on Deformation Measurements*, Orange, California, USA.

Ogaja, C., 2002, *A framework in Support of Structural Monitoring by Real Time Kinematic GPS and Multisensor Data*, Ph.D. NSW, Sydney.

Oral, B., 1994, Global Positioning System (GPS) Measurements in Turkey (1988–1992): Kinematics of the Africa-Arabia- Euraisa Plate Collision Zone, Ph.D. Thesis, Massachusetts Institute of Technology., Cambridge.

Özener, H., A. Doğru, B. Turgut, O. Yılmaz, S. Ergintav, R. Çakmak, U. Doğan and E. Arpat, 2010, "Kinematics of the Eastern Part of the North Anatolian Fault Zone", *Journal of Geodynamics*, Vol. 49, pp. 141–150.

Pearce, J. A., J. F. Bender, S. E. De Long, W. S. F. Kidd, P. J. Low, Y. Güner, F. Saroğlu, Y. Yılmaz, S. Moorbath and J. G. Mitchell, 1990, "Genesis of Collision Volcanism in Eastern Anatolia, Turkey", *Journal of Volcanology and Geothermal Research*, Vol. 44, pp. 189–229.

Pınar, A., Y. Honkura and M. Kikucki, 1996, "A Rupture Model for the 1967 Mudurnu Valley, Turkey Earthquake and its Implications for Seismotectonics in the Western Part of the NAFZ", *Geophysical Research Letters*, Vol. 23, pp. 29–32.

Piper, J. D. A., J. Moore, O. Tatar, H. Gürsoy and R. G. Park, 1996, "Palaeomagnetic Study of Crustal Deformation across an Intracontinental Transform: The North Anatolian Fault Zone in Central Turkey", *Geological Society of London Special Publication*, Vol. 105, pp. 299–310.

Reilinger, R. E., S. C. McCLusky, M. B. Oral, R. W. King and M. N. Toksöz, 1997, "Global Positioning System Measurements of Present-Day Crustal Movements in the Arabia–Africa– Eurasia Plate Collision Zone", *Journal of Geophysical Research*, Vol. 102, pp. 9983–9999.

Reilinger, R., S. McClusky, P. Vernant, S. Lawrence, S. Ergintav, R. Çakmak, H. Özener, F. Kadirov, I. Guliev, R. Stepanyan, M. Nadariya, G. Hahubia, S. Mahmoud, K. Sakr, A. ArRajehi, D. Paradissis, A. Al-Aydrus, M. Prilepin, T. Guseva, E. Evren, A. Dmitrotsa, S. V. Filikov, F. Gomez, R. Al-Ghazzi and G. Karam, 2006, "GPS Constraints on Continental Deformation in the Africa-Arabia-Eurasia Continental Collision Zone and Implications for the Dynamics of Plate Interactions", *Journal of Geophysical Research*, Vol.111, B05411.

Rojay, B., V. Toprak, C. Demirci and L. Süzen, 2001, "Evolution of the Kucuk Menderes Graben (western Anatolia, Turkey)", *Fourth International Turkish Geology Symposium, Çukurova University*, Adana, Turkey.

Rotstein, Y. and A. L. Kafka, 1982, "Seismotectonics of the southern boundary of Anatolia, Eastern Mediterranean Region: Subduction, Collision, and Arc Jumping", *Journal of Geophysical Research*, Vol. 87, pp. 7694–7706.

Salzmann, M., 1990, "MDB: A Design Tool for Integrated Navigation Systems, Kinematic Systems in Geodesy", *Surveying and Remote Sensing Symposium* No. 107, pp. 218–227, Banff, Alberta, Canada.

Saroğlu, F., E. Emre and İ. Kuşçu, 1992, "Active Fault Map of Turkey", *General Directorate of Mineral Research and Exploration*, Ankara.

Şengör, A. M. C. and W. S. F. Kidd, 1979, "Post-Collisional Tectonics of the Turkish-Iranian Plateau and A Comparison with Tibet", *Tectonophysics*, Vol. 55, pp. 361-376.

Şengör, A. M. C. and Y. Yılmaz, 1981, "Tethyan Evolution of Turkey: A Plate Tectonic Approach", *Tectonophysics*, Vol. 75, pp. 181–241.

Şengör, A. M. C., N. Görür and F. Saroğlu, 1985, "Strike-Slip Faulting and Related Basin Formation in Zones of Tectonic Escape: Turkey as a Case Study", *Society of Economic Paleontologists and Mineralogists*, Special Publication, Tulsa, OK.

Şengor, A. M. C., O. Tüysüz, C. İmren, M. Sakınç, H. Eyidoğan, N. Görür, X. Le Pichon and C. C. Rangin, 2005, "The North Anatolian Fault: A New Look", *Annual Review of Earth and Planetary Sciences* Vol. 33, pp. 1–75.

Tatar, O., J. D. A. Piper, H. Gürsoy, A. Heimann and F. Koçbulut, 2004, "Neotectonic Deformation in the Transition Zone between the Dead Sea Transform and the East Anatolian Fault Zone, Southern Turkey: A Palaeomagnetic Study of the Karasu Rift Volcanism", *Tectonophysics* Vol. 385, pp. 17–43.

Taymaz, T., J. Jackson and D. McKenzie, 1991, "Active Tectonic of North and Central Agean Sea", *Geophysical Journal International* Vol. 106, pp. 433–490.

Teunissen, P. J. G. and M. A. Salzmann, 1988, "Performance Analysis of Kalman Filters", *The Faculty of Geodesy, Delft University of Technology*, Netherlands.

Tirifonov, V.G., 1995, "World Map of Active Faults", *Quaternary International* Vol. 25, pp. 3–12.

Tsai, C. and L. Kurz, 1983, "An Adaptive Robustizing Approach to Kalman Filtering", *Automatica*, pp. 279–288.

Vollath U., A. Deking, H. Landau, C. Pagels and B. Wagner, 2000, "Multi-Base RTK Positioning Using Virtual Reference Stations", *International Technical Meeting of the Satellite Division of the Institute of Navigation*, Salt Lake City, Utah, USA.

Vollath U., A. Deking, H. Landau and C. Pagels, 2001, "Long Range RTK Positioning Using Virtual Reference Stations", *Proceedings of the International Symposium on Kinematic Systems in Geodesy*, Banff, Canada.

Wanninger L., 1999, "The Performance of Virtual Reference Stations in Active Geodetic GPS-networks under Solar Maximum Conditions", *Proceedings of the National Technical Meeting of the Satellite Division of the Institute of Navigation*, p. 1419–1427, Nashville, USA.

Wanninger, L., Introduction to Network RTK, http://www.network-rtk.info, 2006.

Wubbena, G., L. Wanninger, A. Bagge and M. Schmitz, 2001, "Network−Based Techniques for RTK Applications", *GPS Society, Japan Institute of Navigation*, pp. 53-65, Tokyo, Japan.

APPENDIX A

In this chapter, 19 CORS-TR reference stations demonstrate three graphs for the coordinate time series of each station beetwen the years of 2009 and 2012. They show significant co-seismic motion and earthquake sequences.

Station velocities were obtained from trend analysis by time series that were formed by daily precise coordinates combined with Kalman analysis

Some information for each of these stations are provided below figures.

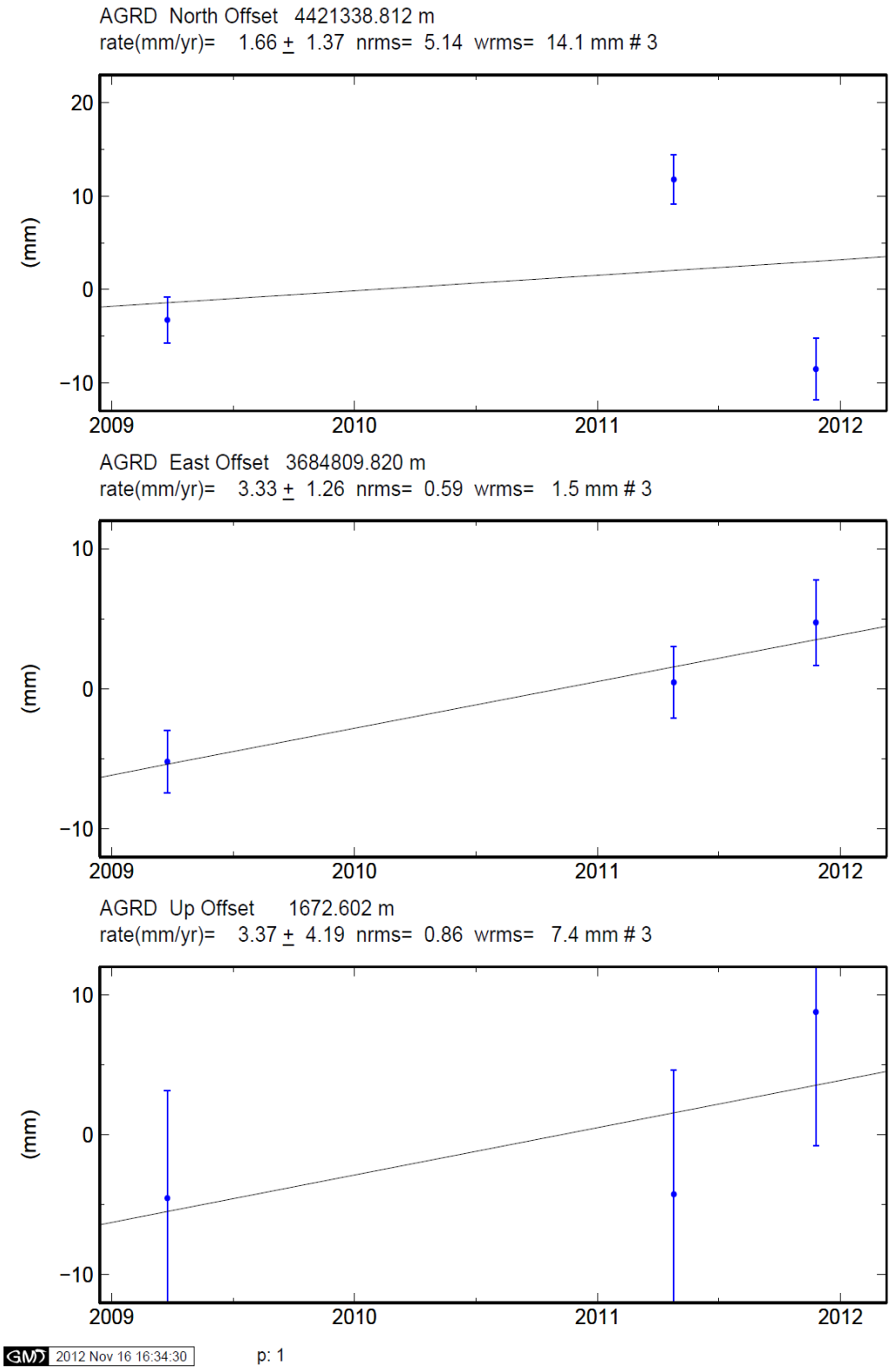

Figure A.1. AGRD station and its coordinate-time series.

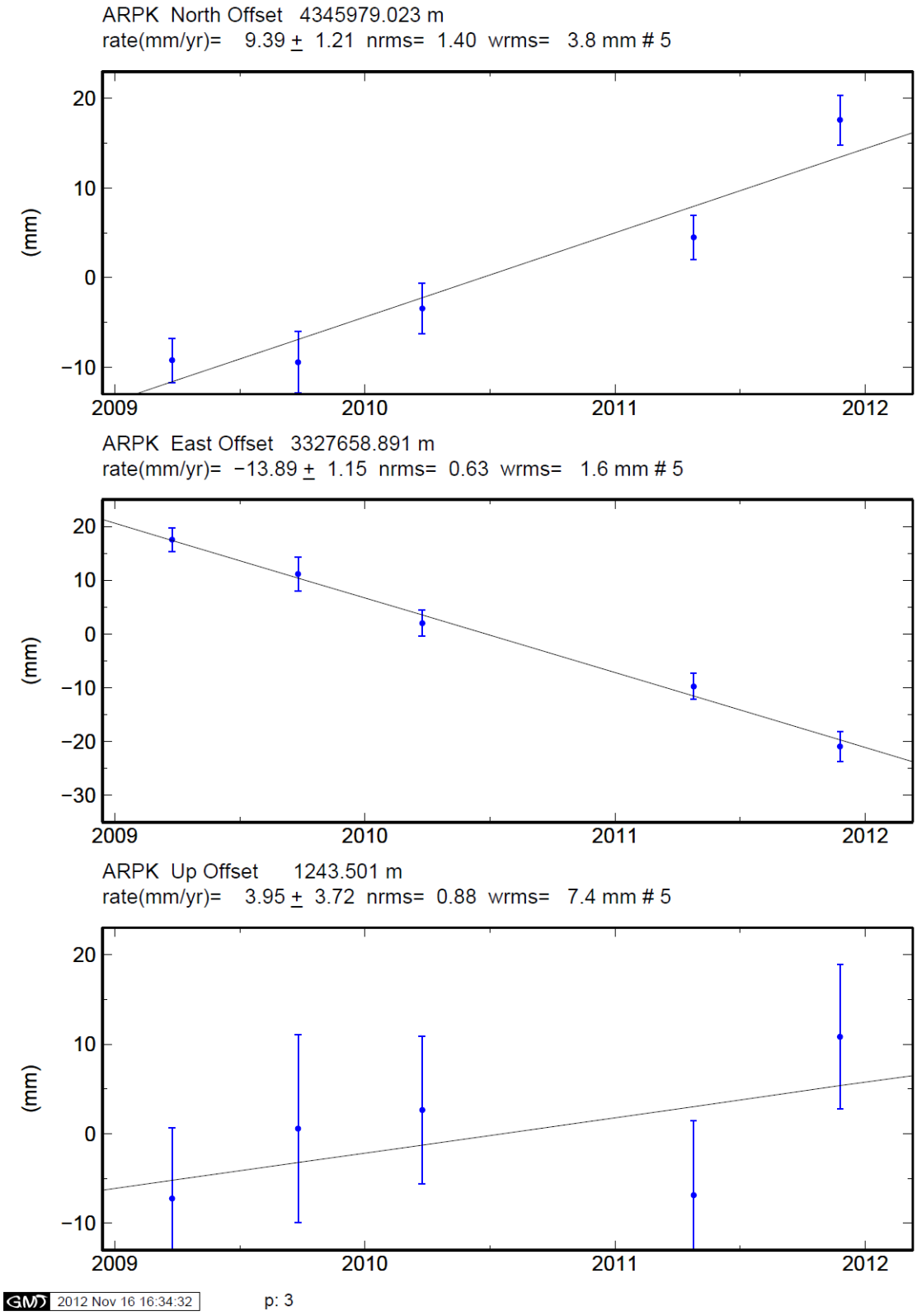

Figure A.2. ARPK station and its coordinate-time series.

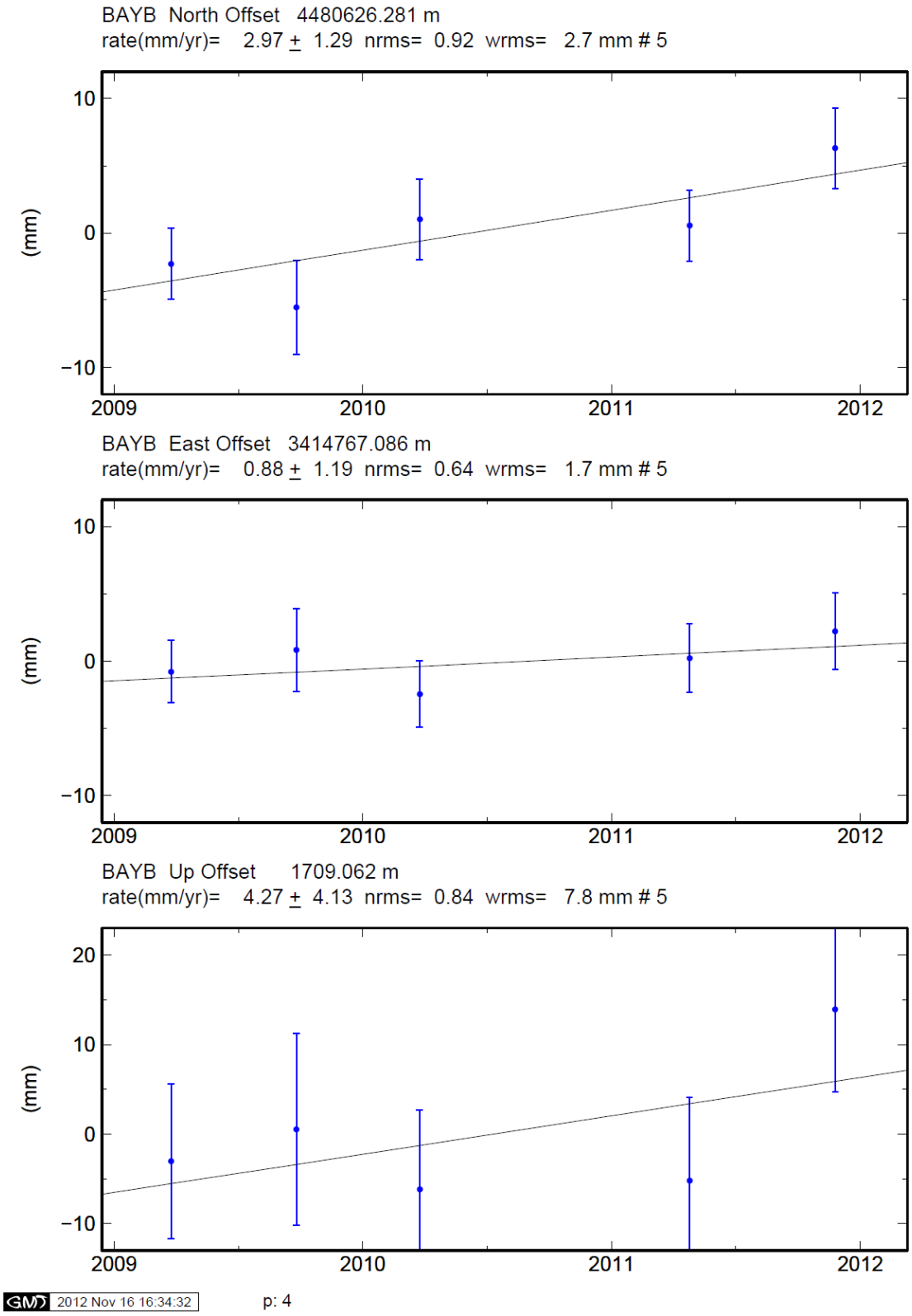

Figure A.3. BAYB station and its coordinate-time series.

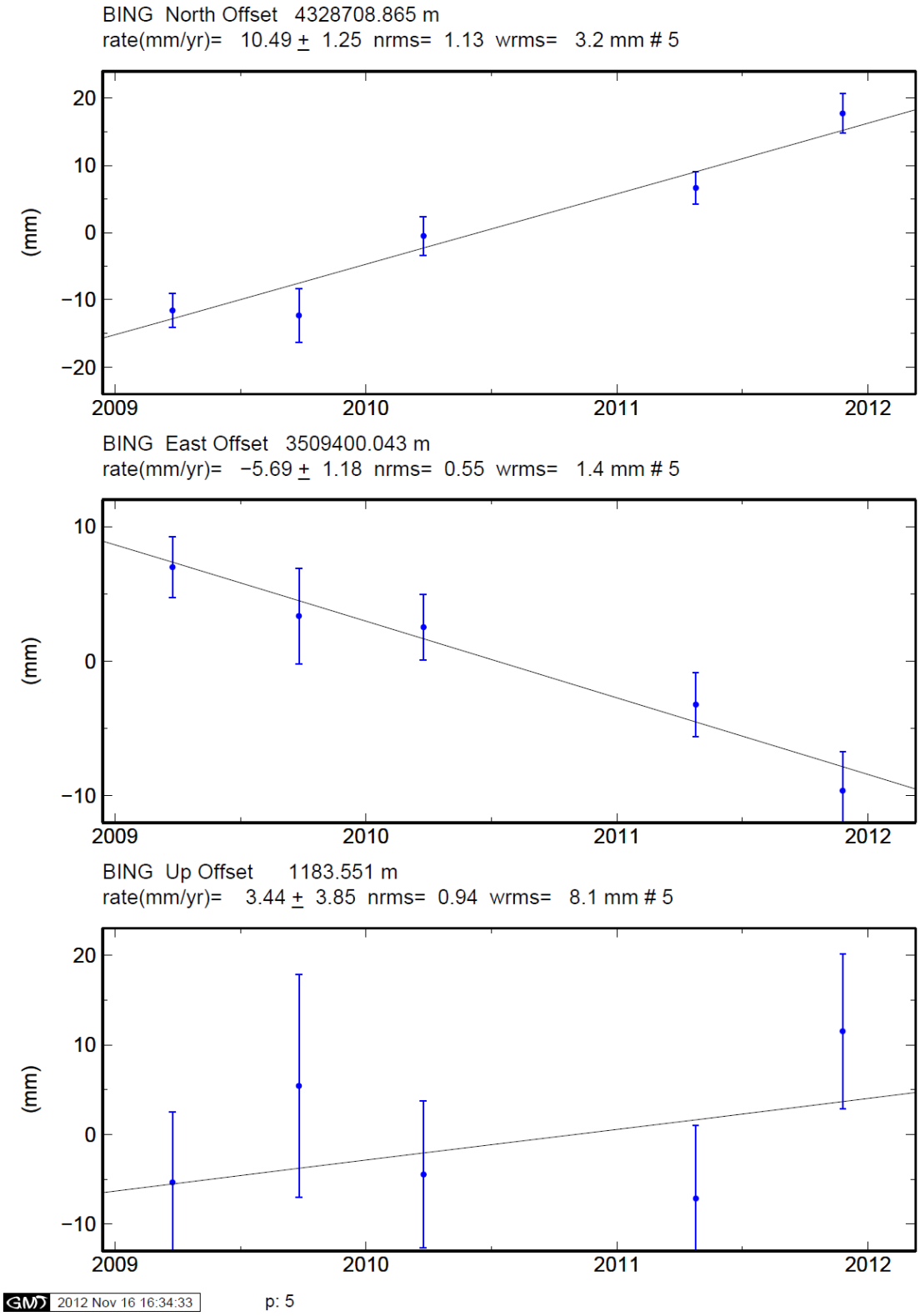

Figure A.4. BING station and its coordinate-time series.

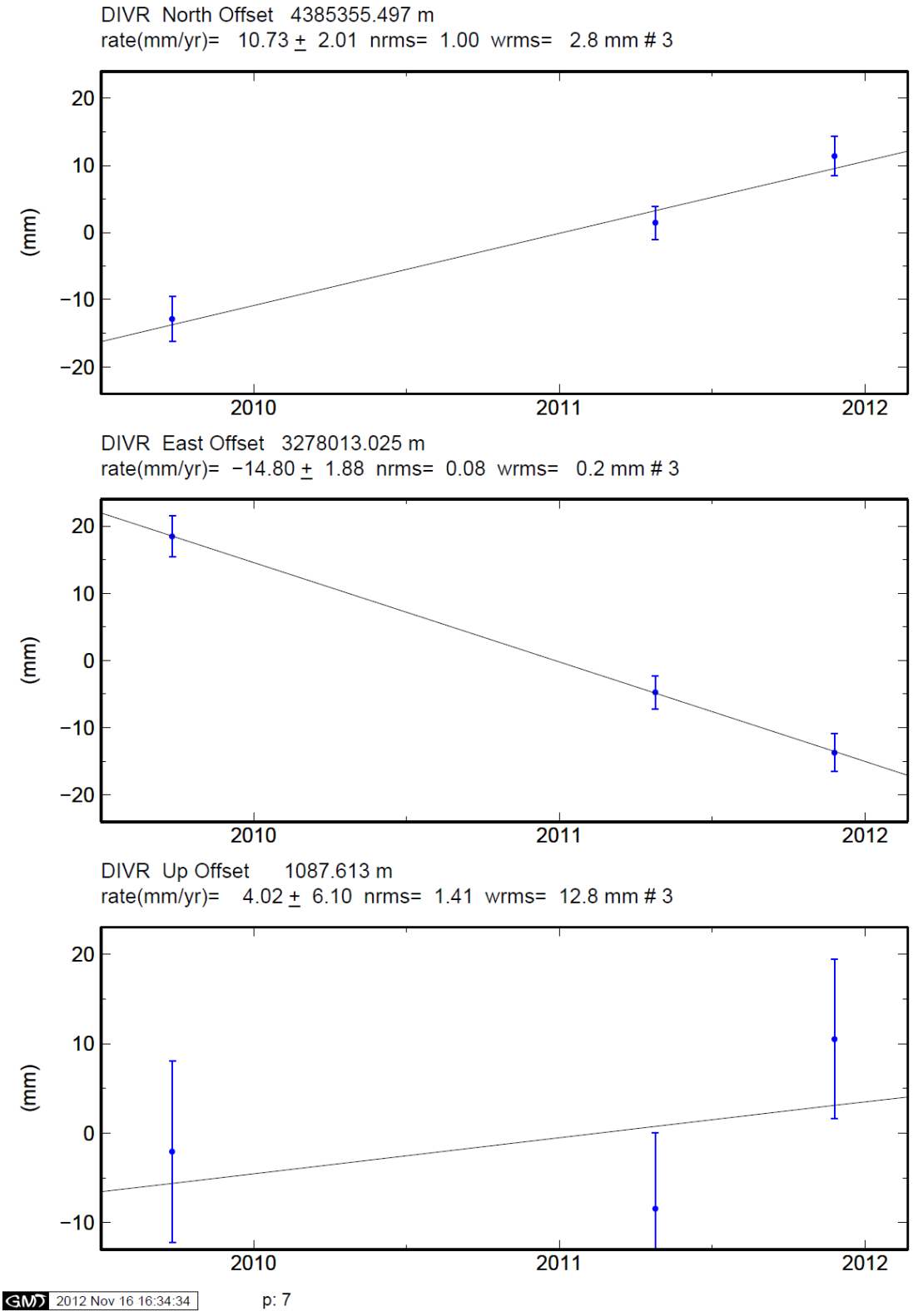

Figure A.5. DIVR station and its coordinate-time series.

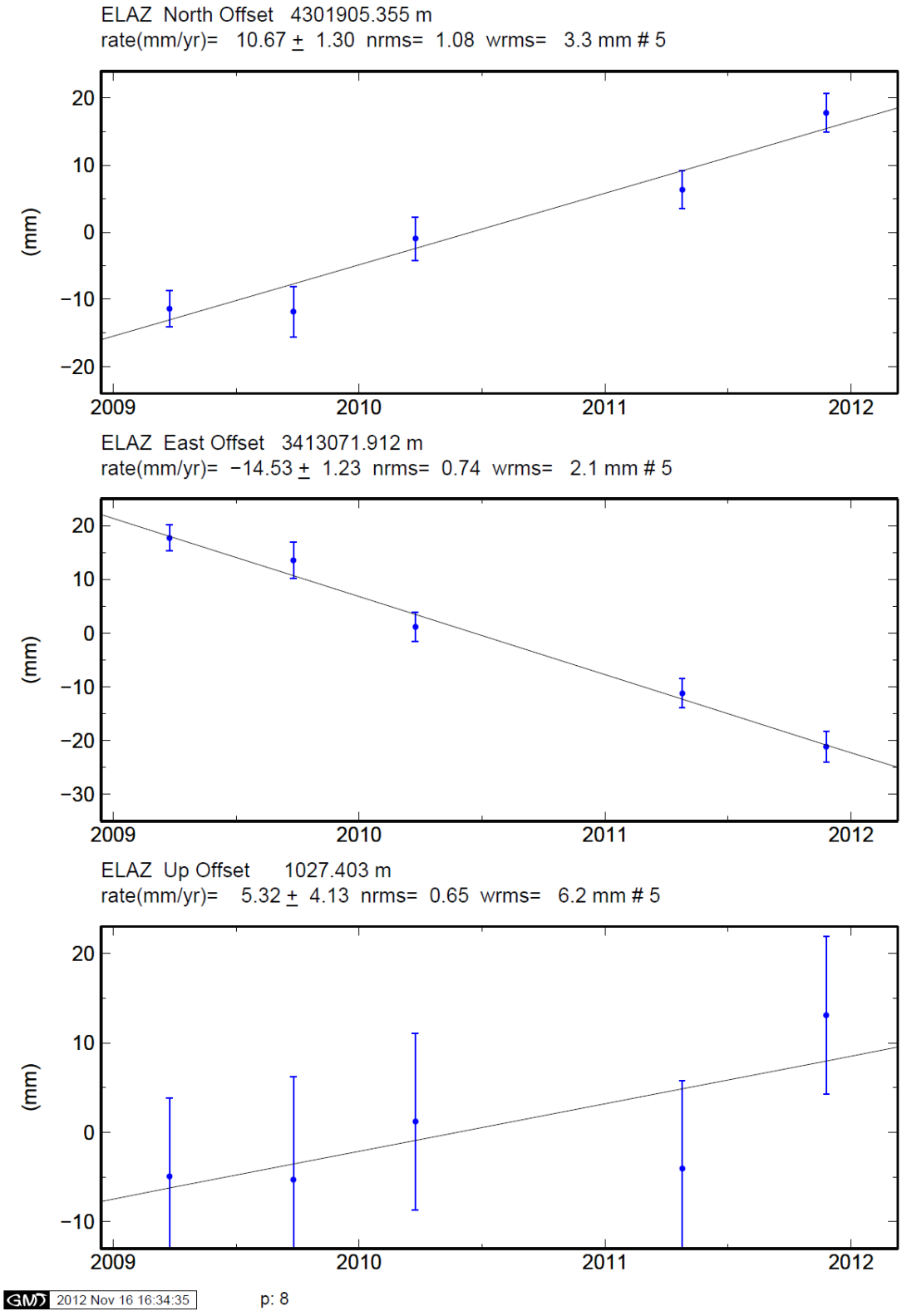

Figure A.6. ELAZ station and its coordinate-time series.

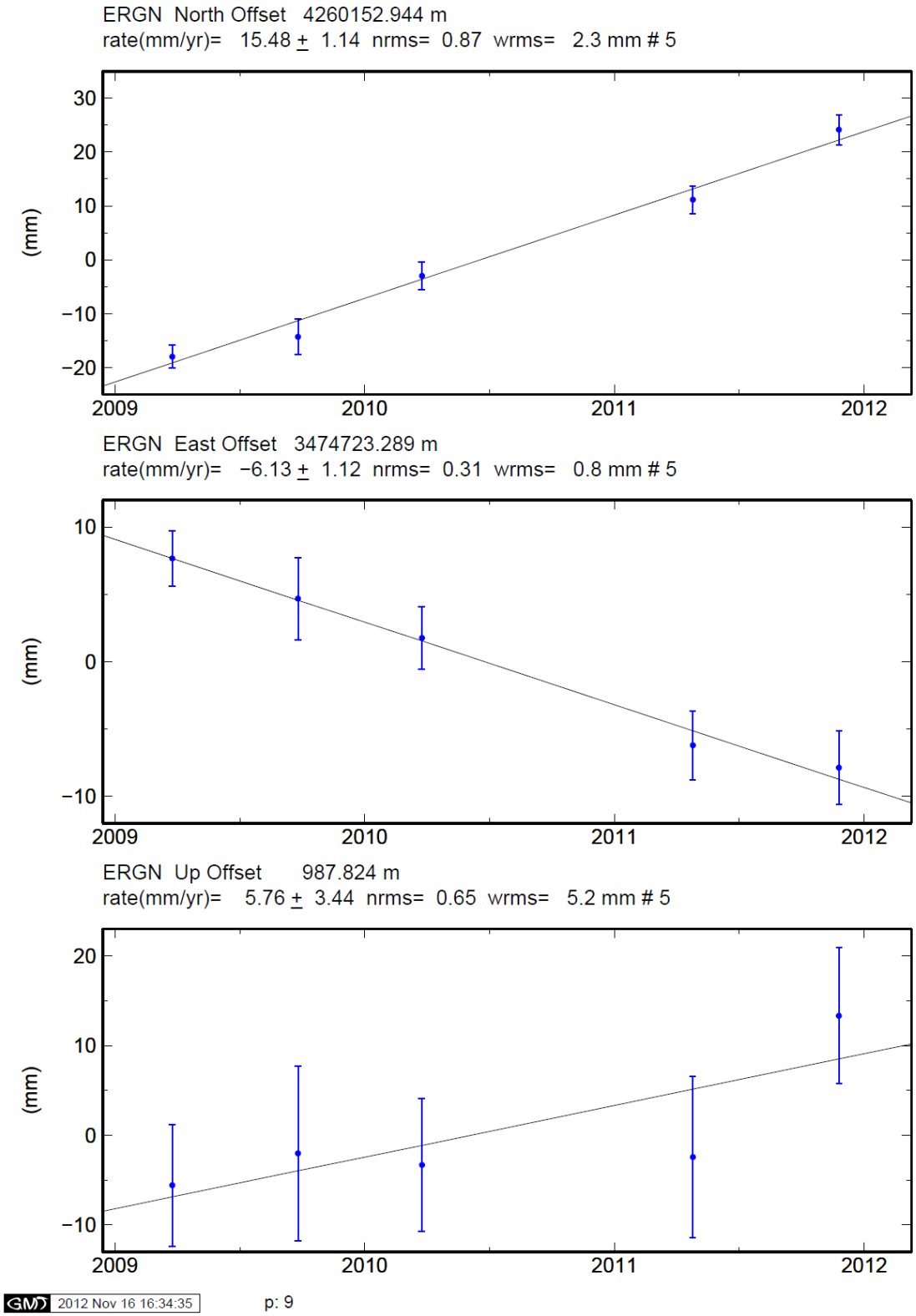

Figure A.7. ERGN station and its coordinate-time series.

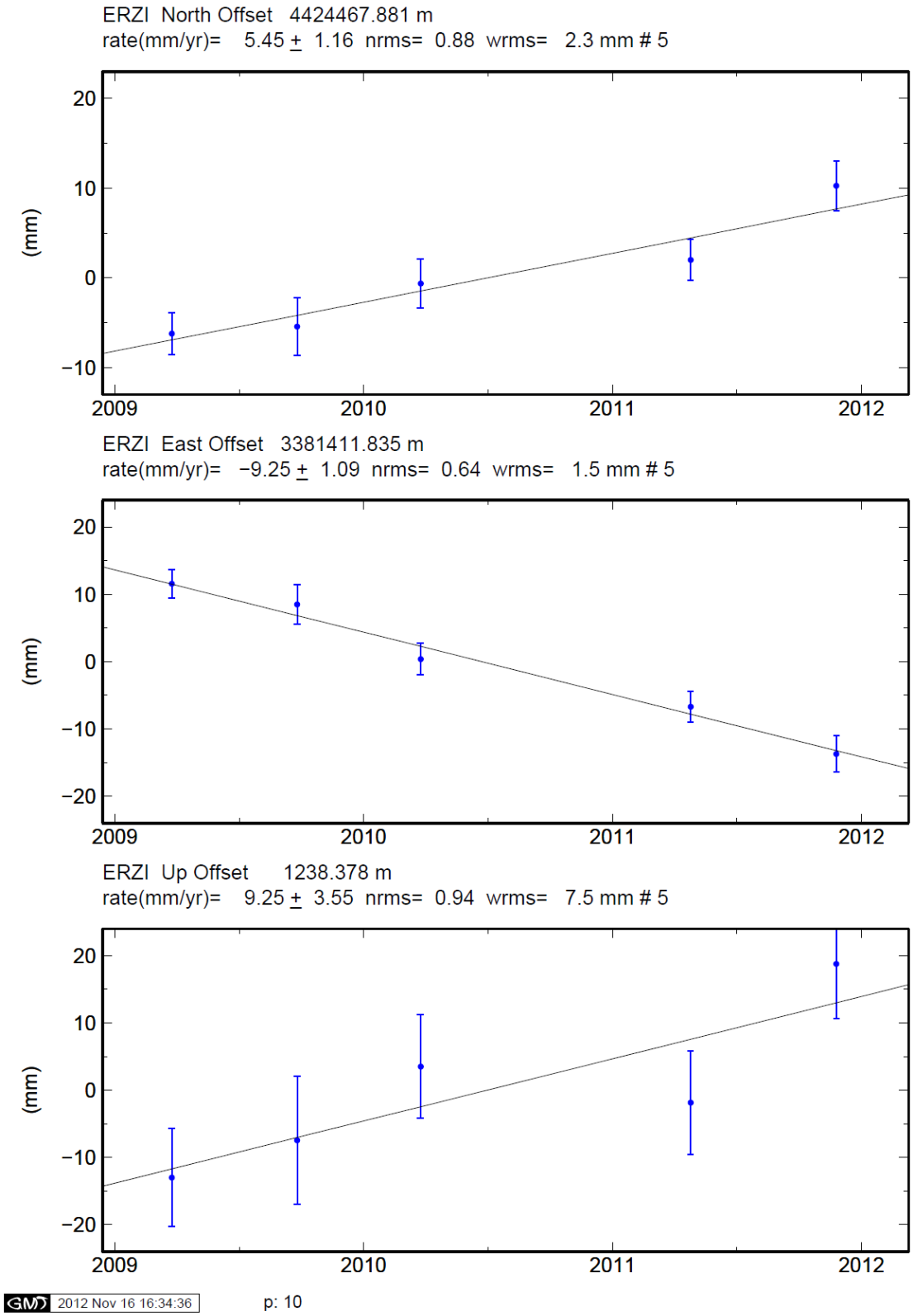

Figure A.8. ERZI station and its coordinate-time series.

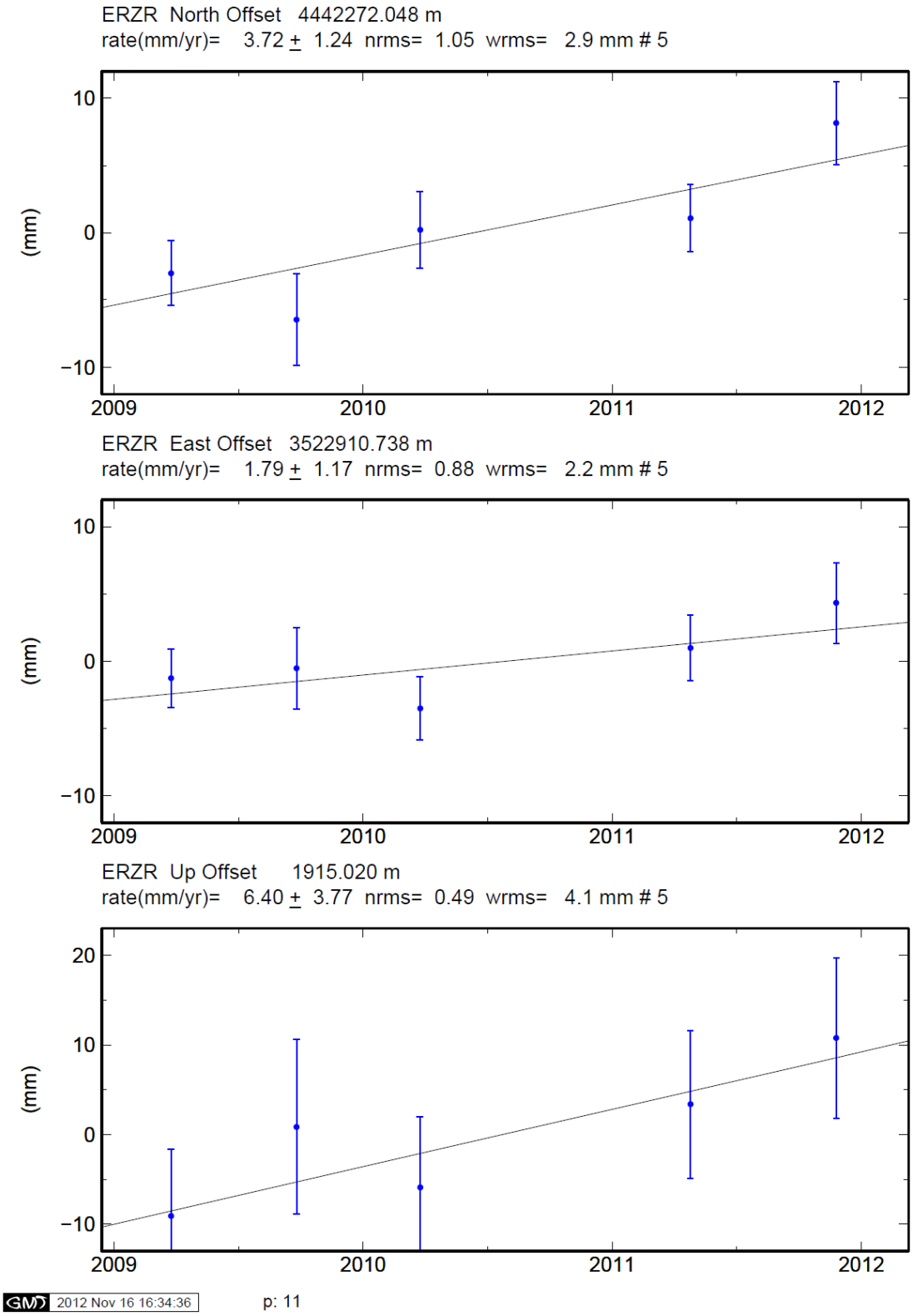

Figure A.9. ERZR station and its coordinate-time series.

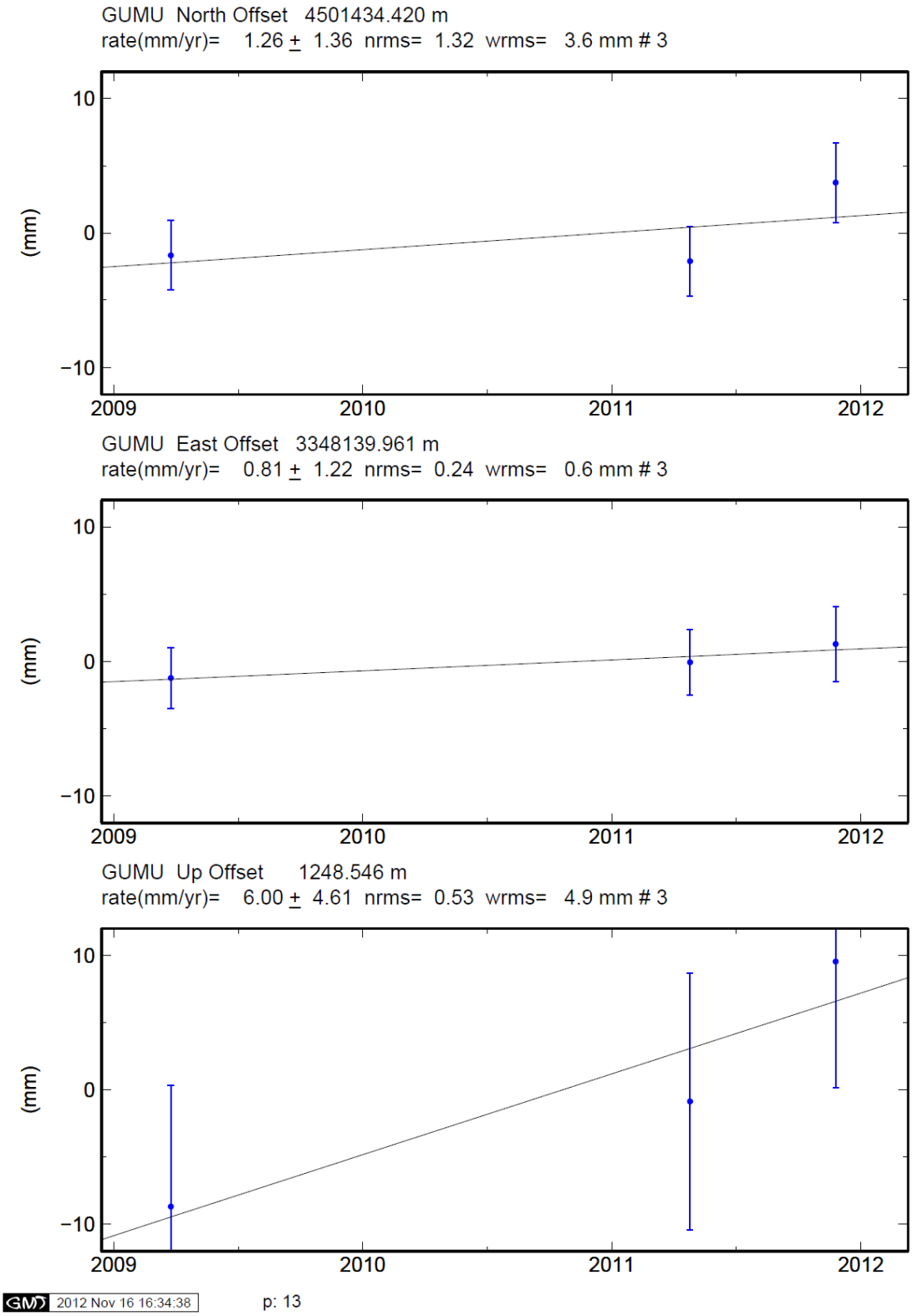

Figure A.10. GUMU station and its coordinate-time series.

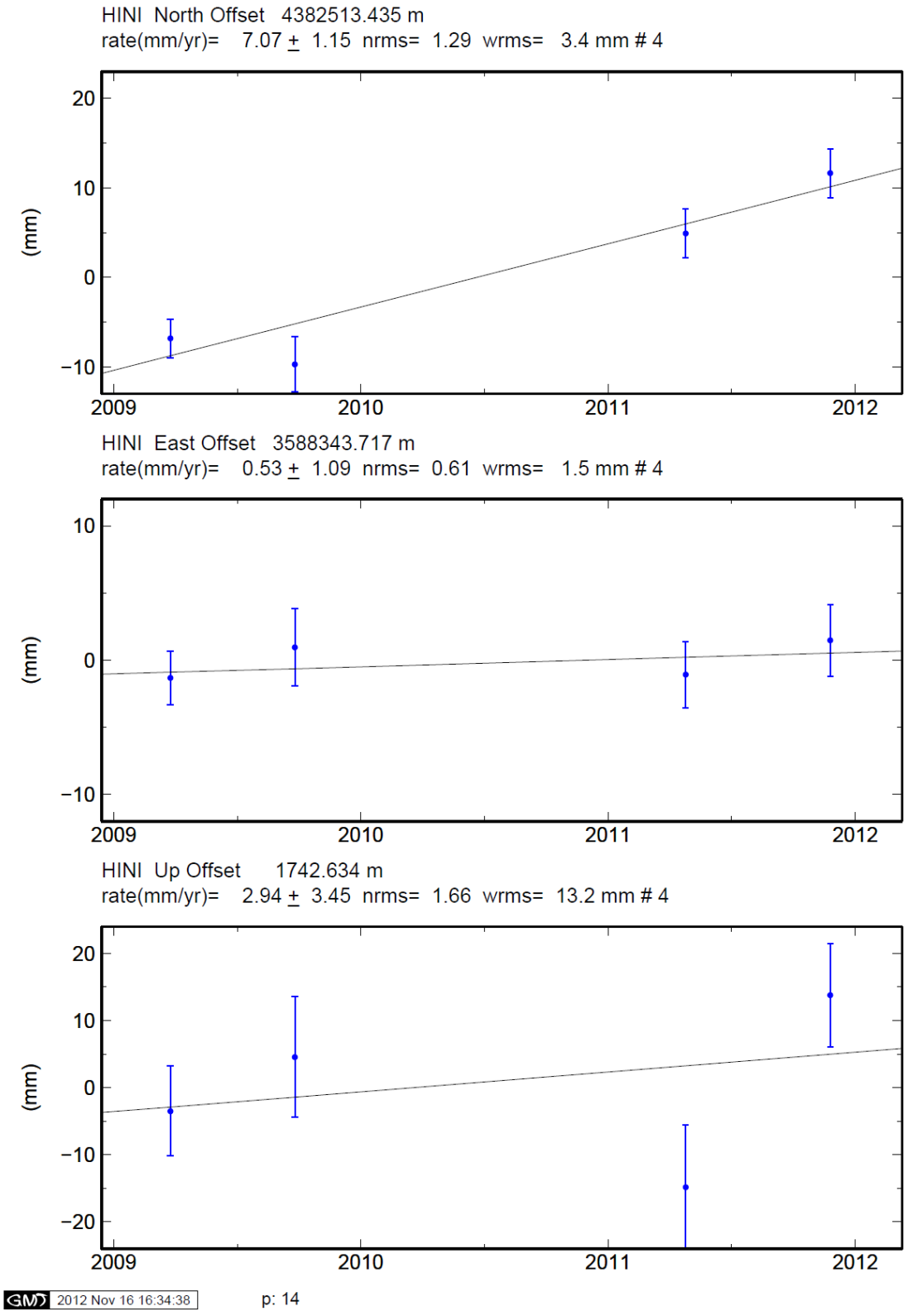

Figure A.11. HINI station and its coordinate-time series.

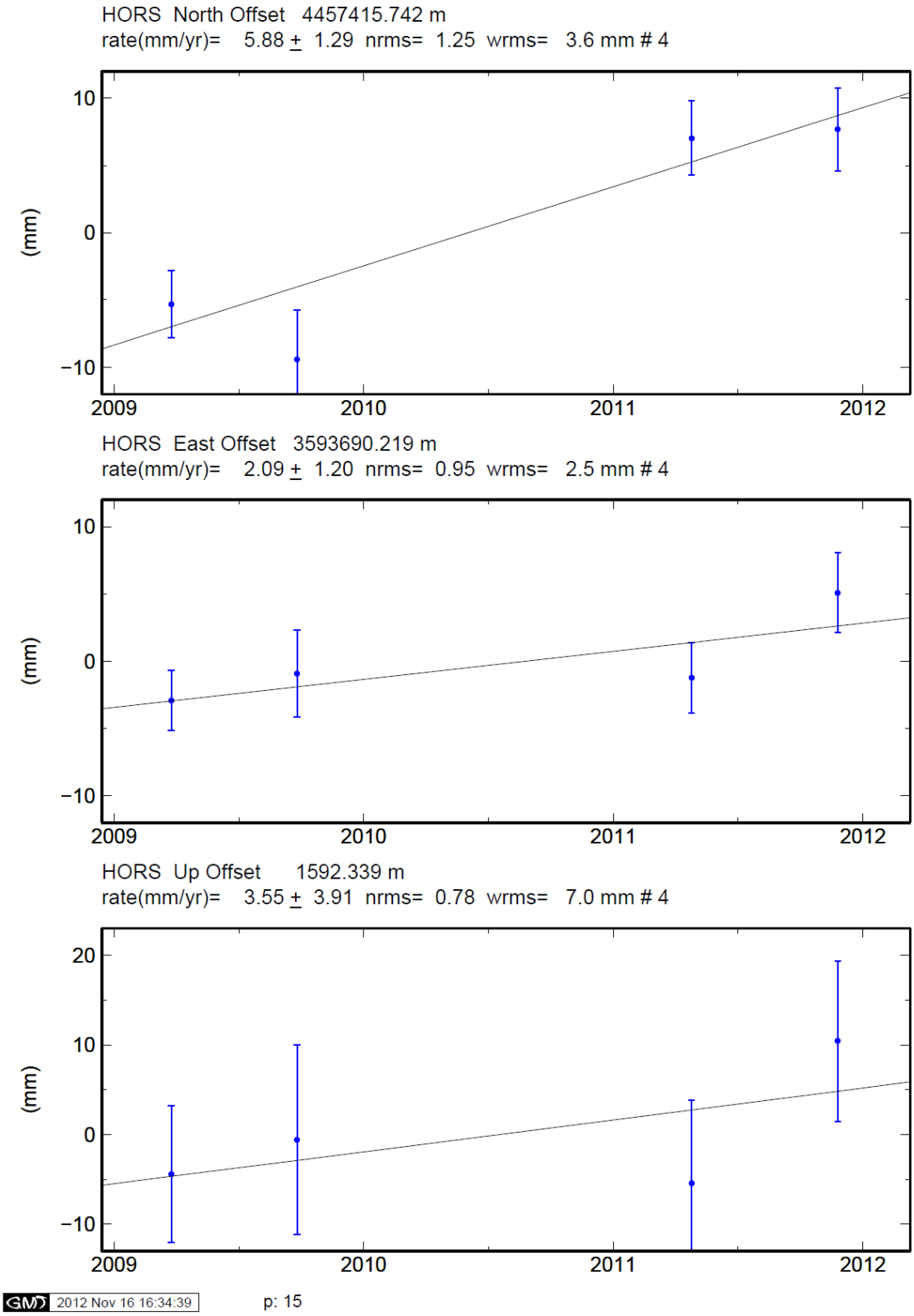

Figure A.12. HORS station and its coordinate-time series.

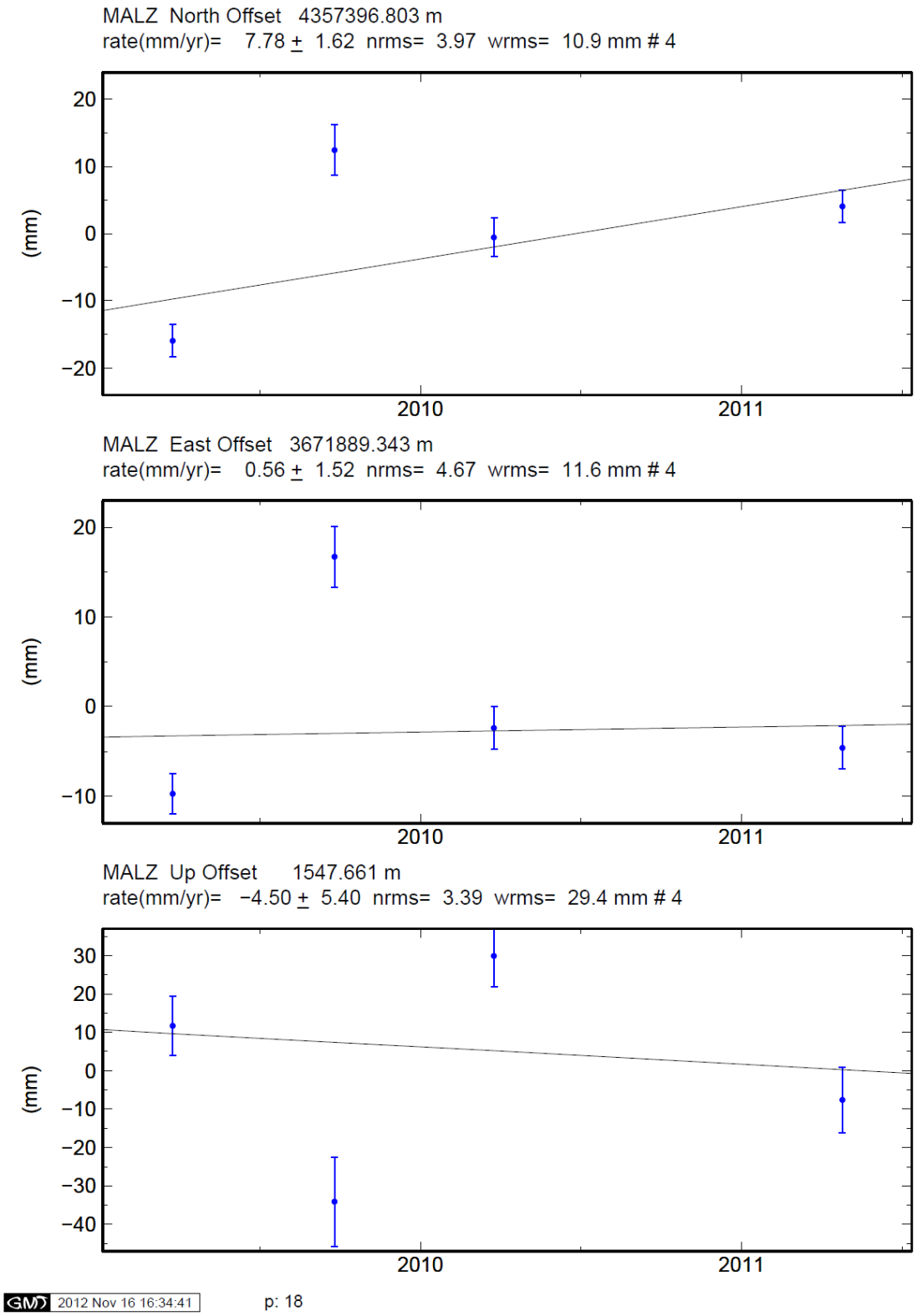

Figure A.13. MALZ station and its coordinate-time series.

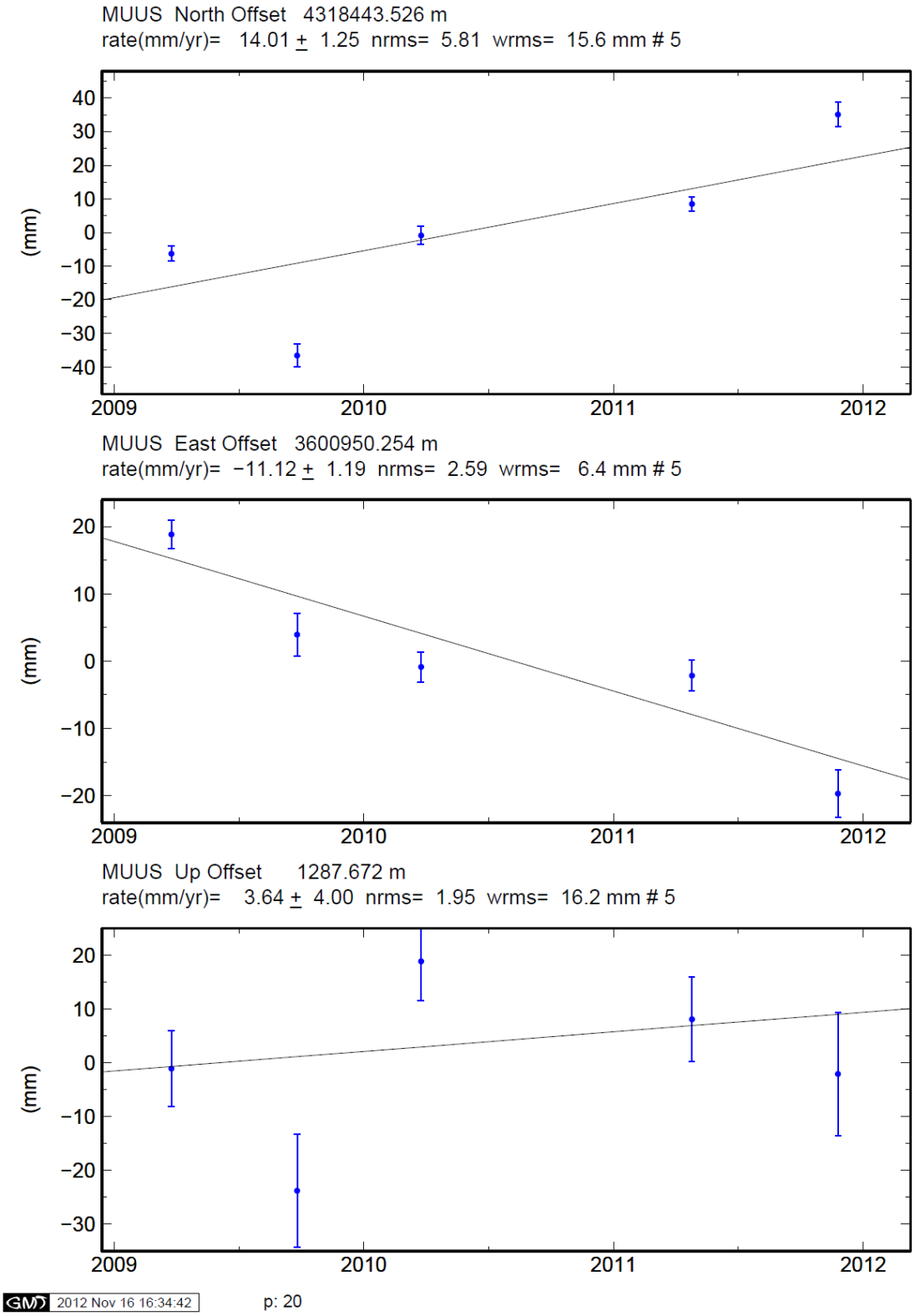

Figure A.14. MUUS station and its coordinate-time series.

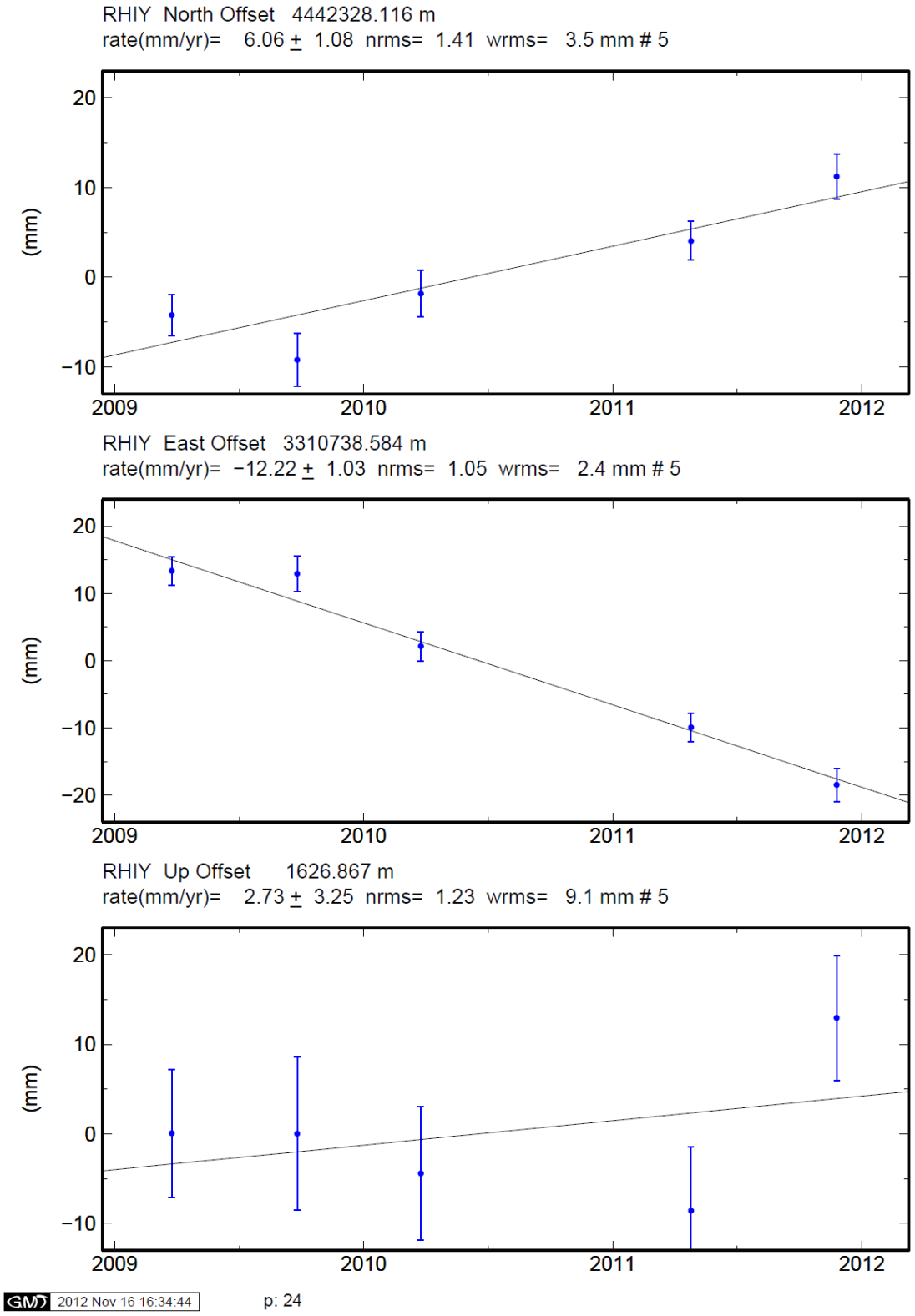

Figure A.15. RHIY station and its coordinate-time series.

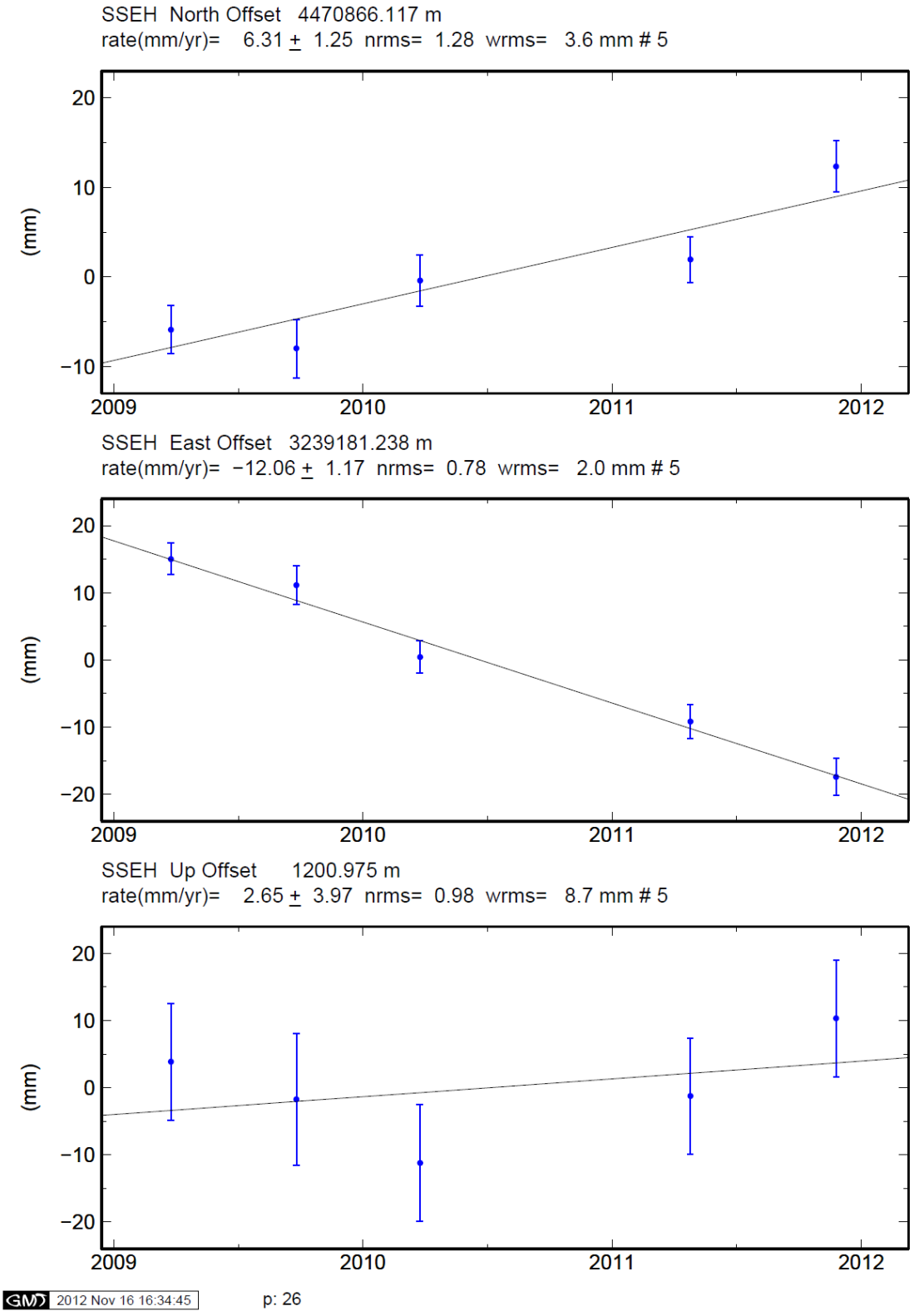

Figure A.16. SSEH station and its coordinate-time series.

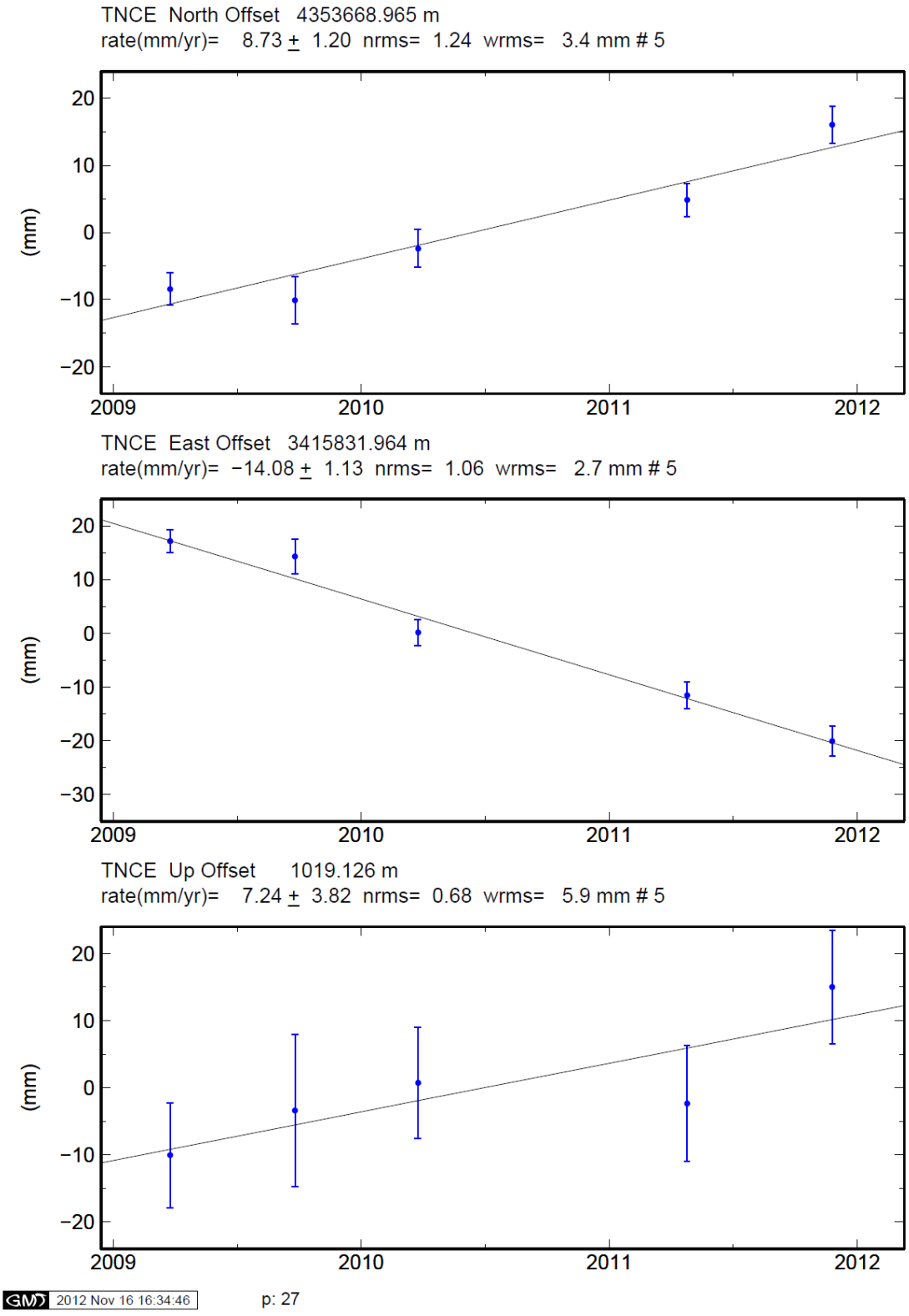

Figure A.17. TNCE station and its coordinate-time series.

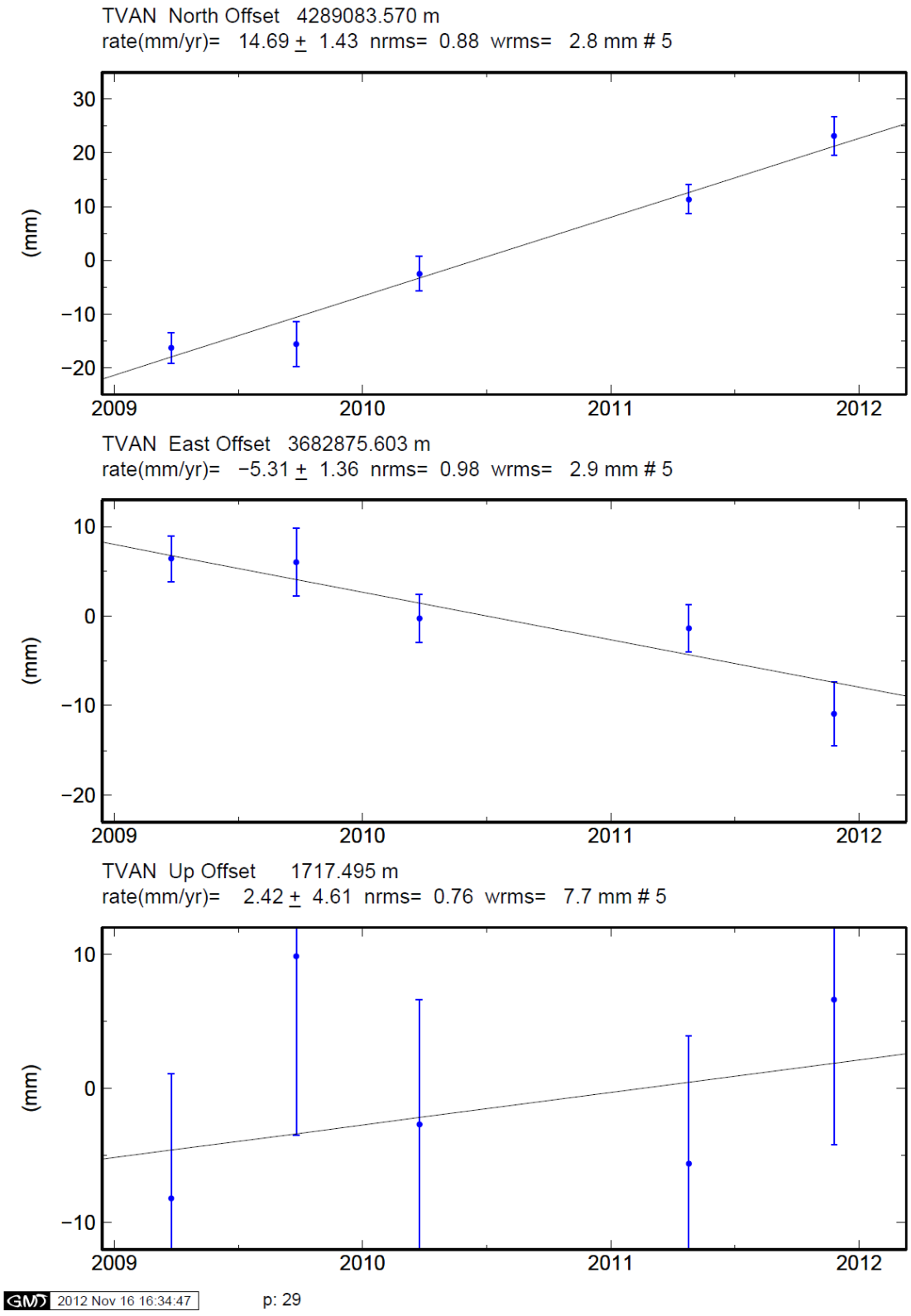

Figure A.18. TVAN station and its coordinate-time series.

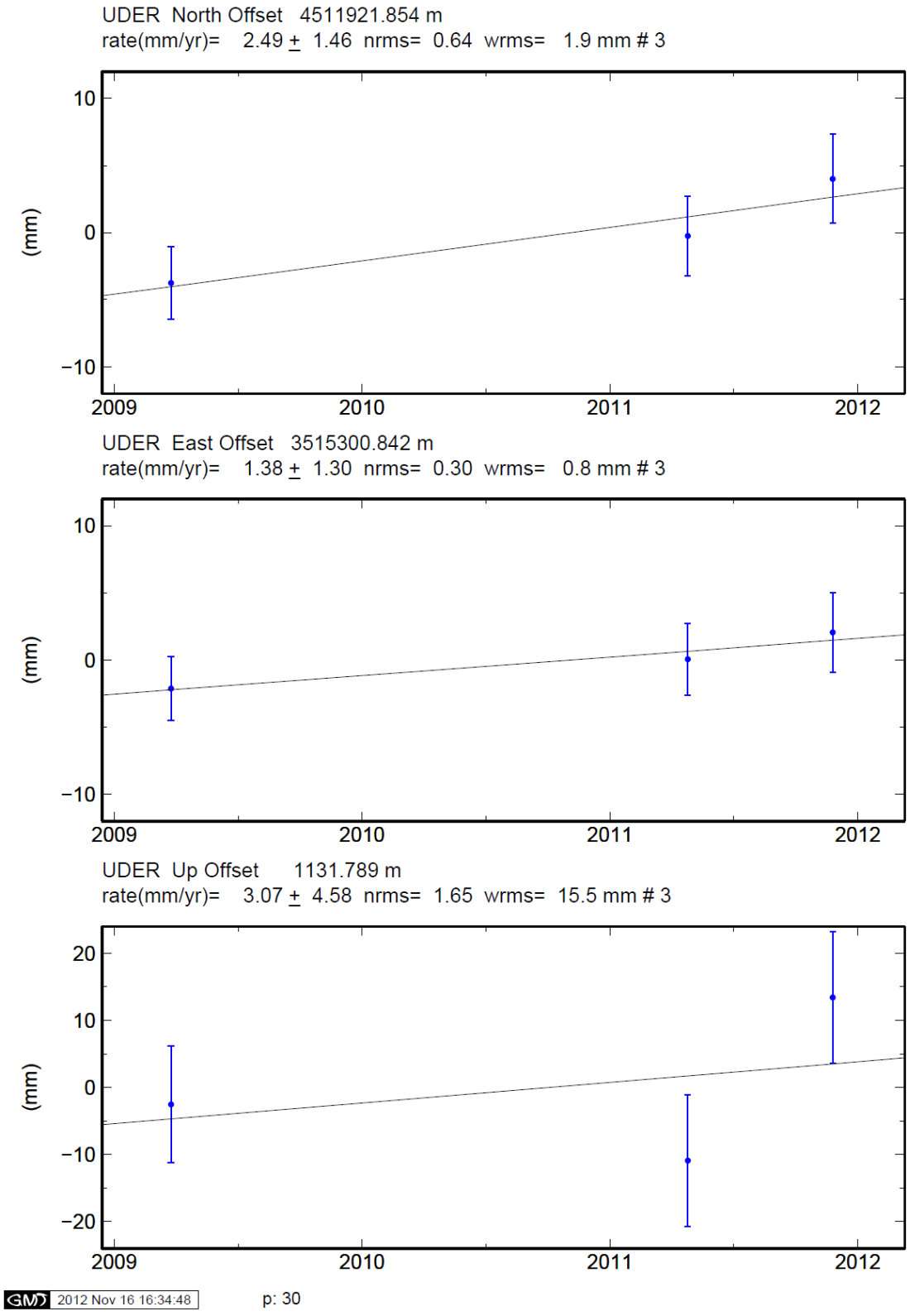

Figure A.19. UDER station and its coordinate-time series.